



**UNIVERSITY OF NAIROBI**

**Investigation of Feed Dynamics using the Radiotracer Residence Time Distribution Method and Metastable Technetium-99: A Case Study of Clinker Milling at National Cement Company, Athi River**

Gitau Jimmy Ndung'u

S56/78895/2015

BSc Industrial Chemistry

A thesis submitted in partial fulfilment of the requirements for the degree of Master of Science in Nuclear Science at the Department of Electrical and Information Engineering, University of Nairobi.

### Declaration

This thesis is my original work and has not been presented for a degree at any other university.

Jimmy Ndung'u Gitau, S56/78895/2015


Signature.....

Date: 27/08/2022.....

### Supervisors' approval

This thesis has been submitted with our knowledge as university supervisors:

- 1) Prof. Michael J. Gatari  
Department of Electrical and Information Engineering  
University of Nairobi, Kenya

Signature.....

**27 August 2022**  
Date: .....

- 2) Michael Mangala  
Department of Electrical and Information Engineering  
University of Nairobi, Kenya

Signature.....

Date: 29th August, 2022.....

## **Dedication**

This study is dedicated to my parents for always urging me to pursue my goals

## **Acknowledgements**

I am grateful to all those, who, in one way or another enabled me to complete this study.

I wish to express my gratitude to my supervisors; Prof. Michael Gatari and Mr. Michael J. Mangala for their keen guidance throughout the whole study.

My heartfelt appreciation goes to all other persons, who assisted me in conducting the study at the National Cement Company, Athi River Plant, including, radiotracer measurements, which were done under challenging conditions. More specifically, the assistance of Mr. David Nganga and Mr. Nelson Rotich, colleagues at the Institute of Nuclear Science & Technology, for participation in field measurements.

I would also like to thank, the International Atomic Energy Agency (IAEA), who offered specialized training on industrial applications of radiotracer techniques, thus providing invaluable knowledge on how to undertake this study. Through the IAEA assistance, I was able to get the assistance of Dr. H. J. Pant, Research Scientist and IAEA consultant, Bhabha Atomic Research Centre, India, who was extremely resourceful in introducing me to potential areas of industrial applications of radiotracer techniques; residence time distribution (RTD) modelling. Dr. Jovan Thereska and Dr. Thorsten Jentsch, both IAEA consultants, offered immense support and assistance in the areas of radiotracer applications.

I am grateful to the staff of National Cement Company Limited, who gave me the opportunity to carry out this study at their plant in Athi River.

I am also thankful to the Nuclear Power and Energy Agency (NuPEA) for awarding me a scholarship to do a Masters' degree program at the Institute of Nuclear Science and Technology, University of Nairobi and the National Research Fund of Kenya for funding this project study.

A big thank you goes out to my family for their unrelenting support, encouragement and constant reminders to complete my thesis research.

## Abstract

In Kenya, cement is a key ingredient in the built and construction industry and in 2017, its production contributed to 5.8% of GDP. In general, cement production is energy intensive and costly. Currently, National Cement Company Limited (NCCL) is the second largest cement producer in Kenya, with an annual production capacity of over 2 million. In 2018, mill 1, its oldest clinker grinding ball mill at their Athi River plant, was suspected to malfunction due to an increase in its power consumption. The mean residence time (MRT) and material hold-up in the mill were also not known. This study, therefore, assessed the flow of porous clinker through the mill to determine if there were any deviations from previously observed models that were affecting its efficiency. This was done using the radiotracer technetium-99m (Tc-99m). Radiotracers are preferred over conventional tracers since they enable online measurement, thereby allowing the system to be studied without interfering with the normal operation of the mill. The radiotracer residence time distribution (RTD) investigation was carried out by introducing clinker labelled with the Tc-99m at the inlet of the mill. Its activity was then monitored at the mill inlet, the mill outlet and at the separator recycle line, using three NaI(Tl) scintillation detectors at each location. The data recorded by the detectors was used to plot the RTD curves, to compute the mean residence time (MRTs) and material hold-up within the clinker ball mill and its separator. The MRT of material within the mill was found to be 980.5 s, whereas the material hold-up was 13.6 tonnes. Further, the empirical RTDs were modelled in DTS PRO software to characterize the flow of material within the ball mill and separator. The results indicated that the flow could be described using two models: an axial dispersion model (ADM) and a tank-in-series model both connected in series to a plug flow component. The two models revealed a significant degree of axial mixing/back-mixing in the ball mill, as indicated by the low pecllet number in the axial dispersion model, and the low value of the number of tanks in the tank-in-series model; this meant that dispersive effects were predominant in the mill resulting in inefficient operation. There were, however, no other flow anomalies observed from the modelling. It is recommended that the operation and design parameters of the ball mill be adjusted to eliminate the observed back-mixing.

## Table of Contents

Declaration.....	ii
Dedication.....	iii
Acknowledgements.....	iv
Abstract.....	v
List of Tables.....	viii
List of Figures.....	ix
List of Abbreviations.....	x
CHAPTER ONE: INTRODUCTION.....	1
1.1    Background to the Study.....	1
1.2    Statement of the Problem.....	3
1.3    Main Objective.....	3
1.3.1    Main Objective.....	3
1.3.2    Specific Objectives.....	3
1.4    Justification and Significance of the Study.....	4
1.5    Scope of the Study.....	4
CHAPTER TWO: LITERATURE REVIEW.....	5
2.1    Theory of Radiotracer Technology.....	5
2.1.1    Introduction.....	5
2.1.2    Radiotracer Techniques in Industry.....	5
2.2    RTD Measurements.....	6
2.3    Selection of Radiotracers for Industrial Applications.....	9
2.3    Detectors and Modelling Software.....	12
2.4    Review of Studies On Application of Radiotracers in Industry: Residence Time Distribution Method.....	13
2.5    Research Gaps.....	14
CHAPTER THREE: MATERIALS AND METHODS.....	16
3.1    Study Location and Facility.....	16
3.2    Radiation Safety and Personnel Exposure Monitoring.....	17
3.3    Radiotracer measurements: Materials and Instrumentation.....	18
3.3.1    Instrumentation.....	18
3.3.2    Radiotracer Material and Preparations.....	19
3.3.3    Field Radiotracer RTD Measurements.....	21
3.3.4    Data Treatment and Analyses.....	23
3.4    Flow model Simulation: DTS PRO software.....	23

3.4.1	Perfect Mixer .....	25
3.4.2	Perfect Mixers in Series .....	25
3.4.3	Perfect Mixers in Series with Back-mixing .....	25
3.4.4	Perfect Mixers in Series with a Dead Volume .....	25
3.4.5	Plug flow model.....	26
3.4.5	Plug flow open to diffusion model.....	26
CHAPTER FOUR: RESULTS AND DISCUSSION .....		29
4.1	Introduction.....	29
4.2	Results of RTD and MRT Measurements.....	29
4.3	Flow model Simulation: DTS PRO software.....	33
CHAPTER FIVE: CONCLUSIONS AND RECOMMENDATIONS .....		37
5.1	Conclusions.....	37
5.2	Recommendations.....	37
References.....		38

### **List of Tables**

Table 2.1 Examples of radiotracers induced through neutron activation of solid materials....	11
Table 2.2 Examples of aqueous radiotracer solutions used in surface labelling .....	12
Table 4.1: Total counts recorded at the ball mill outlet vs total counts at the recycle outlet of the separator .....	29
Table 4.2: Experimental MRTs and hold-up .....	33
Table 4.3: A comparison of the experimental RTD measurements and the flow modelling results .....	35



## List of Figures

Figure 1.1: The cement production process .....	2
Figure 2.1: measurement of flowrate using a radiotracer .....	6
Figure 2.2: diagram showing RTD determination by instantaneous injection of a tracer as described in the DTS Pro instruction manual .....	7
Figure 2.3: A plot of tracer concentration at the outlet versus time .....	8
Figure 2.4: RTD curves with different standard deviations.....	9
Figure 3.1: A map showing the location of the.....	16
Figure 3.2: The dosimeter used by the author, showing the effective dose at the end of the investigation.....	18
Figure 3.3: Thallium-activated sodium iodide detectors (a) and Connecting cable 50m long (b).....	19
Figure 3.4: Laptop placed on top of the Altaix Data Acquisition System.....	19
Figure 3.5: Schematic diagram of a typical technetium-99m generator (Hidayati, 2016) .....	20
Figure 3.6: Ball mill in closed circuit mode .....	21
Figure 3.7: The point of introduction of the tracer - the conveyor at the inlet of the ball mill .....	22
Figure 3.8: The interior of the second chamber of the clinker ball mill .....	22
Figure 3.9: Detector D3 with a lead collimator at the recycle line from the separator.....	23
Figure 3.10: Perfect mixing models.....	24
Figure 3.11: Plug flow models.....	24
Figure 3.12: Perfect mixers in series with dead volume .....	26
Figure 3.13: The DTS Pro software user interface .....	27
Figure 4.1(a), (b), (c): uncorrected radiotracer concentration curves from the 1 <sup>st</sup> run for detectors; D1, D2 and D3.....	30
Figure 4.2(a), (b), (c): uncorrected radiotracer concentration curves from the 2 <sup>nd</sup> run for detectors D1, D2 and D3.....	31
Figure 4.3: Variations of corrected and normalized radiotracer concentration responses at D1, D2, and D3 for the 1st run (a), and the 2nd run (b). .....	32
Figure 4.4: Block diagram of Model-1 .....	34
Figure 4.5: Block diagram of Model-2 .....	34
Figure 4.6: Comparison of experimental and model simulated RTD curves (Run 1) .....	36
Figure 4.7: Comparison of experimental and model simulated RTD curves (Run 2) .....	36

## List of Abbreviations

<b>ADM</b>	Axially dispersed model
<b>cps</b>	Counts per second
<b>CNSC</b>	Canadian Nuclear Safety Commission
<b>D1</b>	Detector positioned at the outlet of the ball mill
<b>D2</b>	Detector positioned at the inlet of the ball mill
<b>D3</b>	Detector positioned at outlet 2 (recycle line) of the cyclone separator
<b>DAS</b>	Data Acquisition System
<b>DTS Pro</b>	Residence Time Distribution (Distribution des Temps de Séjour in French) Professional software
<b>GDP</b>	Gross domestic product
<b>IAEA</b>	International Atomic Energy Agency
<b>keV</b>	Kiloelectron-Volt
<b>KNBS</b>	Kenya National Bureau of Statistics
<b>kWh</b>	Kilowatt-hour
<b>MBq</b>	Megabequerel
<b>MRT</b>	Mean Residence Time
<b>μSv</b>	Microsieverts
<b>NaI(Tl)</b>	Sodium iodide doped with thallium
<b>NCCL</b>	National Cement Company Limited
<b>OPC</b>	Ordinary pozzolana cement
<b>PPC</b>	Portland pozzolana cement
<b>RMS</b>	Root mean square
<b>RTD</b>	Residence Time Distribution
<b>Tc-99m</b>	Metastable technetium-99

# CHAPTER ONE: INTRODUCTION

## 1.1 Background to the Study

Cement is defined as a hydraulic binder material that when mixed with water sets, hardens and aggregates (Hewlett, 2003). It is used in making concrete; one of the most used construction materials in the world in the built industry (Goncalves and Margarido, 2015). Types of cement include Portland cement, calcium sulphate plasters, sorel cement and sodium silicate (Bye, 1999). Portland cement is predominantly used globally for building and construction (Bye, 1999). It is a type of cement primarily made up of calcium silicates, calcium aluminate, calcium aluminoferrite and gypsum a hydrated calcium sulphate (Hewlett, 2003).

The production of Portland cement can be summarized in two major steps, namely: First, limestone and clay are ground and blended, then, fed into a kiln, where they are heated to produce clinker. Secondly, the clinker, which is in the form of hard nodules, is ground together with gypsum in a mill, to yield the fine powder that is cement (Goncalves and Margarido, 2015). The last step is clinker milling, where the clinker nodules are ground together with gypsum into a fine powder of particles less than 100 microns in size and a surface area of 330 to 380 m<sup>2</sup>/Kg (Bye, 1999). The fineness of the particles is a critical parameter that governs the quality of the cement, as it affects its hydration and consequently its setting and hardening (Hewlett, 2003). Ball mills are usually used for grinding the clinkers to obtain fine cement powder. A ball mill for clinker grinding is a rotating cylinder that usually consists of two chambers separated by a diaphragm. The first chamber is for crushing the clinker, whereas, the second chamber is for fine grinding. The first chamber contains large grinding media that can crush the large-sized nodules of the clinker and the second chamber contains smaller grinding media for fine grinding (Alsop et al., 2007).

Cement production is an energy-intensive process with the clinker milling consuming the most electrical power (Worrell and Galitsky, 2008). Optimizing these processes presents a significant cost-saving opportunity in the manufacturing process of cement.

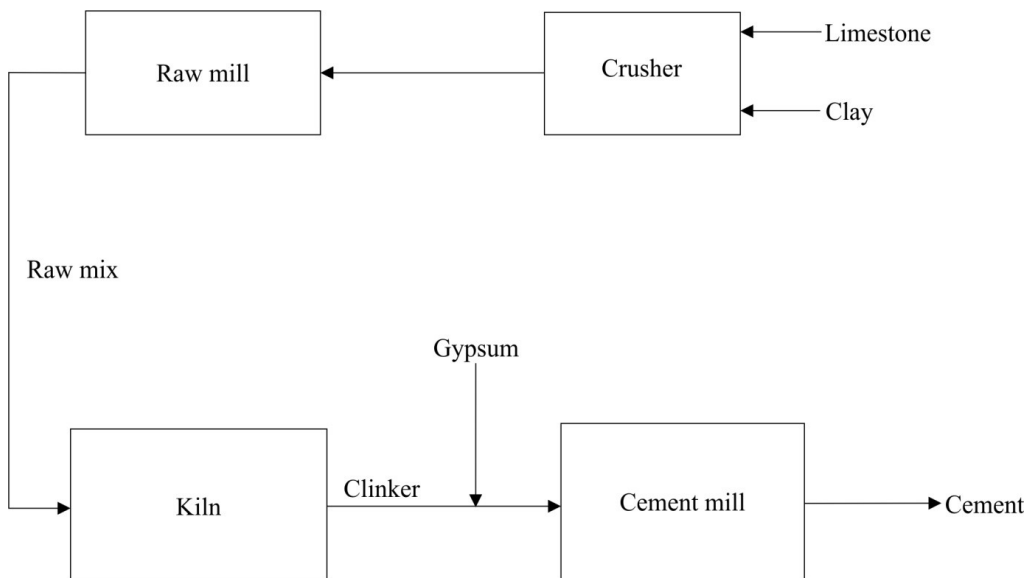


**Figure 1.1: The cement production process** (Olsen et al., 2010)

The National Cement Company Limited, NCCL, is currently the second largest cement producer in Kenya, with an annual production capacity of over 2 Million tonnes and markets its products in the east African region (Oxford Business Group, 2016). NCCL produces two different types of cement; Simba Cement, 32.5R, a Portland Pozzolana Cement (PPC) and Simba Power 42.5R, an Ordinary Portland Cement (OPC). The raw materials used in the manufacture of both types of cement are clinker and gypsum; however, in the manufacture of PPC, pozzolana is also added. The pozzolana added to PPC gives it resistance to calcium hydroxide, an alkali which forms when cement is mixed with water, by reacting with it (Bye, 1999). This leads to further cementation, reduced leaching in the concrete and resistance to sulphate, chloride and alkali attacks; Overall, PPC produces more durable concrete when compared to OPC.

In the production of Portland Pozzolana Cement, the raw material, composed of 60% clinker, 35% pozzolana and 5% gypsum, is fed into the mill at a rate of 50 tonnes per hour. Additionally, the mill is then set to rotate at 19 rpm, and the material is expected to have a residence time of 10 minutes, according to the design specifications. The product from the mill outlet is fed to a separator where the coarse particles are separated from the fine particles. After separation, the coarse particles are then returned to the mill inlet, for further grinding, whereas the finer particles are stored and packaged as cement. However, according to NCCL Production Reports (2018), the oldest clinker mill, Mill 1, had developed malfunctions, which resulted in an unexplained increase trend in specific power consumption. Several diagnostics attempts have proved futile and unsuccessful.

It has been shown elsewhere, that radiotracers can be used to study and diagnose industrial processes without disturbing the system operations (Fogler, 2016; Adzaklo et al., 2016; Charlton, 2012). A radiotracer RTD study is done by introducing a suitable radioisotope at the inlet of an industrial process and monitoring the detector response to the isotope at the outlet (IAEA, 2008). The signal recorded can give valuable

information about the process under study including any malfunctions that might be present. In Kenya, RTD measurements have been used to investigate the efficiency of a ball mill; however, this has been done using chemical tracers (Makokha et al., 2014). In a recent study of the residence time distribution of a mill, Makokha et al. (2014), used sodium chloride as a chemical tracer, which required them, to manually sample and test the mill discharge periodically, to determine tracer concentration, which would have otherwise been done using radiotracer in-situ detection measurements. Mumuni et al. (2011), used a radiotracer RTD study to determine the efficiency of two clinker grinding mills in Ghana, while they were in operation.

## **1.2 Statement of the Problem**

Anomalies in the flow of material through clinker ball mills can result in reduced efficiency (Adzaklo et al., 2016). These can be investigated using radiotracer residence time distribution studies, which have been used to characterize and evaluate the flow of the feed material through ball mills (Mumuni et al., 2010), for optimization. In Kenya, however, radiotracer techniques are yet to be introduced for industrial applications, and in particular, in the manufacture of cement.

The average power consumption for the ball mill in this study had shown an increasing trend in power consumption, rising from an average of 34 kWh/ton in February 2018 to 41 kWh/ton in September 2018 (NCCL, 2018). There was a need to determine if there was any deviation, from the ideal flow pattern of the clinker feed in the ball mill, that was causing the increased power consumption. There was also, no information available on the mill's mean residence time and material hold-up in the mill. In practice, solids hold-up, a parameter that indicates the amount of feed within the mill at a given time, is essential in evaluating whether the clinker mill is operating optimally (Rogers and Austin, 1984).

## **1.3 Main Objective**

### **1.3.1 Main Objective**

To assess the feed dynamics of the clinker milling process at the NCCL Athi River plant using the residence time distribution method and Tc-99m as the radiotracer.

### **1.3.2 Specific Objectives**

- i) To conduct a radiotracer Residence Time Distribution study of the clinker grinding ball mill using Technitium-99m;
- ii) To determine the mean residence time and the material hold-up in tonnes of the clinker grinding ball mill.
- iii) To describe and model the material flow pattern in the clinker grinding mill and separator using the RTD data and DTS Pro software;

#### **1.4 Justification and Significance of the Study**

Conventional tracers are impractical for use in the diagnosis of full-scale industrial systems because of their many constraints. When compared to radiotracers, chemical tracers and dyes require much larger quantities to be detected (IAEA, 2008). Conventional tracers require physical sampling of the material under study; for industrial processes using closed vessels and pipes, this would require stopping the process. Radiotracers, on the other hand, have been extensively used to optimize manufacturing and other industrial processes by providing a means to investigate and troubleshoot reactors with minimal disturbance. Radiotracers are preferred for their high sensitivity, and are widely used for online diagnosis of large-scale systems; They are therefore ideal for assessing the effectiveness of the clinker milling process (IAEA, 2011).

Radiotracers enable in-situ, online measurement which provides details in the shortest duration possible, more so, radiotracers that emit gamma radiation can be detected through radiation transmission. The emission of gamma radiation is not affected by the presence of other materials in the system. Gamma radiation can be detected through the walls of vessels, provided the energy is high enough. As a consequence, appropriately selected radiotracers do not interfere with the process activities and are ideal for use in the assessment of dynamic processes.

Cement industries will benefit from the convenience of radiotracer studies when used to assess material flow dynamics and troubleshoot processes. Clinker grinding, which is the focus of this study, has been singled out as consuming the most electrical energy in Portland cement manufacture (Worrell and Galitsky, 2008).

This study will demonstrate the effectiveness of radiotracer RTD studies, as a viable method of troubleshooting in cement manufacturing processes and for other industrial process applications in the country.

#### **1.5 Scope of the Study**

The selected ball mill for this study is located at National Cement Company Limited, Athi River, Machakos County. It is representative of other ball mills being utilized in other cement plants in Kenya. The study covered the movement of the clinker feed from the inlet of the ball mill, through the outlet of the mill, and the return of coarse particles through the recycle line of the separator. The investigation also included modelling of the RTD data measured by the detectors to determine the flow models that suitably describe the feed dynamics within the mill and separator. The models used were therefore limited to those available in the DTS Pro software and their combinations.

The literature review examined the scientific principles of radiotracer technology and residence time distribution studies. The author further established considerations made when selecting radiotracers. Research gaps in previous work in radiotracer RTD were identified, specifically in industrial applications.

## CHAPTER TWO: LITERATURE REVIEW

### 2.1 Theory of Radiotracer Technology

#### 2.1.1 Introduction

Radioisotopes have in the past few decades, found widespread use in the study of physical, chemical and biological systems. In their application in industry, radioisotopes are used either as sealed sources or as radiotracers. A tracer is any material whose nuclear, atomic, chemical or physical properties enable the identification, observation and following of physical, chemical and biological processes (IAEA, 2008). Radioactive tracers or radiotracers, in short, can be traced through a system because of the radiation they emit from their radioactive decay. As a result, radiotracer studies in industry allow for in situ and non-invasive optimization and troubleshooting of processes. This means that a process can be evaluated without incurring any downtime.

Radiotracers are chosen over conventional tracers, such as chemical tracers and dyes, for industrial tracer studies due to several inherent advantages. These include high detection sensitivity, in-situ detection, physicochemical compatibility and limited memory effect (Othman and Kamarudin, 2014). Exceedingly small amounts of a radiotracer can produce sufficient radiation for detection during tracer studies. Gamma radiation can be transmitted through vessel walls, this enables the study of processes using gamma-emitting radiotracers without stopping or interfering with operations (IAEA, 2008). Radiotracers are not affected by the physical conditions of the system such as heat, pressure or colour of the material (Thýn and Žitný, 2002). Since significantly smaller amounts are needed for a study compared to other tracers, a radiotracer can be introduced into a system without disturbing the system's dynamics (IAEA, 2008).

These advantages have led to the use of radiotracer technology in a wide range of industries including mineral grinding and enrichment (IAEA, 2008; Vinnett et al., 2018), fertilizer production (Abdelouahed et al., 2018), chemical manufacturing (Charlton, 1984; Pant et al., 2001), wastewater treatment (De Clercq et al., 2005; Adwet et al., 2019), paper production (Sheoran et al., 2016), nuclear power production (Pant et al., 2015), oil exploration (Bjørnstad et al., 1990) and petroleum refining (IAEA, 2008).

#### 2.1.2 Radiotracer Techniques in Industry

Radiotracer applications in industry typically involve the injection and subsequent monitoring of the radioactive material in the process under investigation (Charlton, 1984). The movement of the radiotracer in the process pipes and vessels is monitored by measuring its activity using radiation detectors installed at strategic locations. This movement is representative of the flow of the process material and provides important information on the dynamics of the process.

Charlton (1984) discusses leak detection, measurements of flow rate, and residence time distribution studies as some of the applications of radiotracers in industry. The researcher gives an example of leak detection in a distiller, where the coolant is suspected to be leaking into the product stream. A radiotracer may be injected into the coolant, and a detector placed downstream on the product line. Detection of the radiotracer in the product stream would confirm leakage, and its concentration is used to ascertain the rate of leakage. To measure the flow rate of a fluid in a pipe, a radiotracer is instantaneously injected into the pipe such that its activity is detected as a sharp pulse by two detectors downstream (IAEA, 2004; Kasban et al, 2010). The distance,  $d$ , between the detectors is measured before injection, and the time difference,  $t$ , between the two recorded pulses is noted. If the internal radius of the pipe,  $r$ , is known, the flow rate of the fluid,  $u$ , can then be calculated as follows:

$$u = \frac{d\pi r^2}{t} \quad (2.1)$$

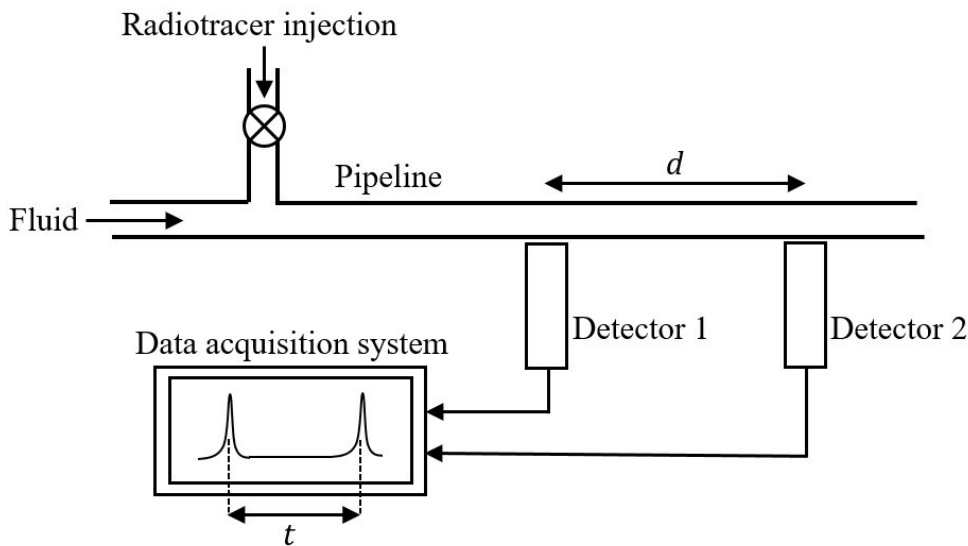


**Figure 2.1: measurement of flowrate using a radiotracer (Charlton, 1984)**

The radiotracer technique of measuring flow rate may be necessary when a flow meter is unavailable, faulty or needs to be calibrated. It can also be useful when monitoring the partitioning of flow into multiple streams and in the calculation of mass balance throughout a plant or processing unit.

## 2.2 RTD Measurements

An important concept in the study of industrial processes is that of Residence Time Distribution (RTD). The RTD of a chemical reactor refers to the distribution of time taken by the particles of a fluid through a reactor (Fogler, 2016). As such, it is a probability distribution of time taken by a fluid in the reactor vessel. In this case, ‘reactor’, may refer to a chemical reactor, mixer, grinder or any other process. The RTD is measured by introducing tracer materials at the inlet of a reactor and monitoring the response of the tracer at the outlet



as shown in figure 2.2. A curve of tracer concentration at the outlet against time is then plotted to obtain the residence time distribution as indicated in figure 2.3.

According to the IAEA (2008), the RTD function is calculated from the normalization of the area under the RTD curve as shown in equation (1);

$$E(t) = \frac{c(t)}{\int_0^{\infty} c(t) dt} \quad (2.1)$$

where  $E(t)$  is the RTD function and  $C(t)$  is the tracer concentration at the outlet.  $E(t)$  is thus a fraction of the injected tracer leaving the reactor at a given time. When a radiotracer is used  $C(t)$  is the net count rate.

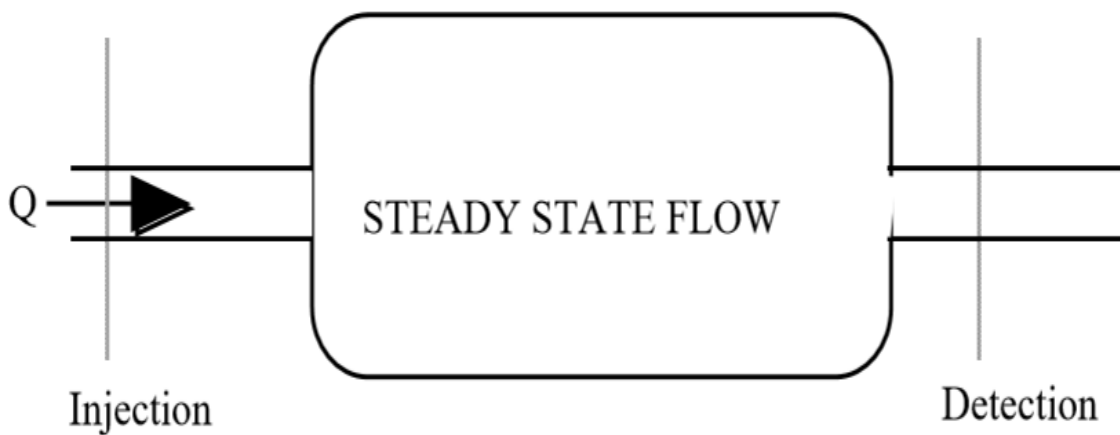


**Figure 2.2: diagram showing RTD determination by instantaneous injection of a tracer as described in the DTS Pro instruction manual ( PROGEPI/SYSMATEC, 2000)**

It follows that the fraction of material leaving the reactor between time  $t = 0$  and  $t = \infty$  is 1;

$$\int_0^{\infty} E(t) dt = 1 \quad (2.2)$$

The RTD of a reactor varies depending on its performance. This is because the flow dynamics of the fluid through the reactor will influence the RTD data recorded at the outlet. Consequently, comparing RTD data of a real (non-ideal) reactor with that of an ideal reactor enables one to diagnose the reactor operation (Fogler, 2016).

The Mean Residence Time (MRT) and the standard deviation of the RTD curve, are critical in studying the behaviour of the fluid through the reactor. The theoretical MRT is given by equation (2.3):

$$\tau = \frac{V}{Q} \quad (2.3)$$

where  $\tau$  is the theoretical mean residence time,  $V$  is the reactor volume and  $Q$  is the flow rate. Experimentally the MRT is given by:

$$\tau_a = \frac{\int_0^{\infty} tE(t) dt}{\int_0^{\infty} E(t) dt} = \int_0^{\infty} tE(t) dt \quad (2.4)$$

where  $\tau_a$  is the mean residence time determined from the experiment.

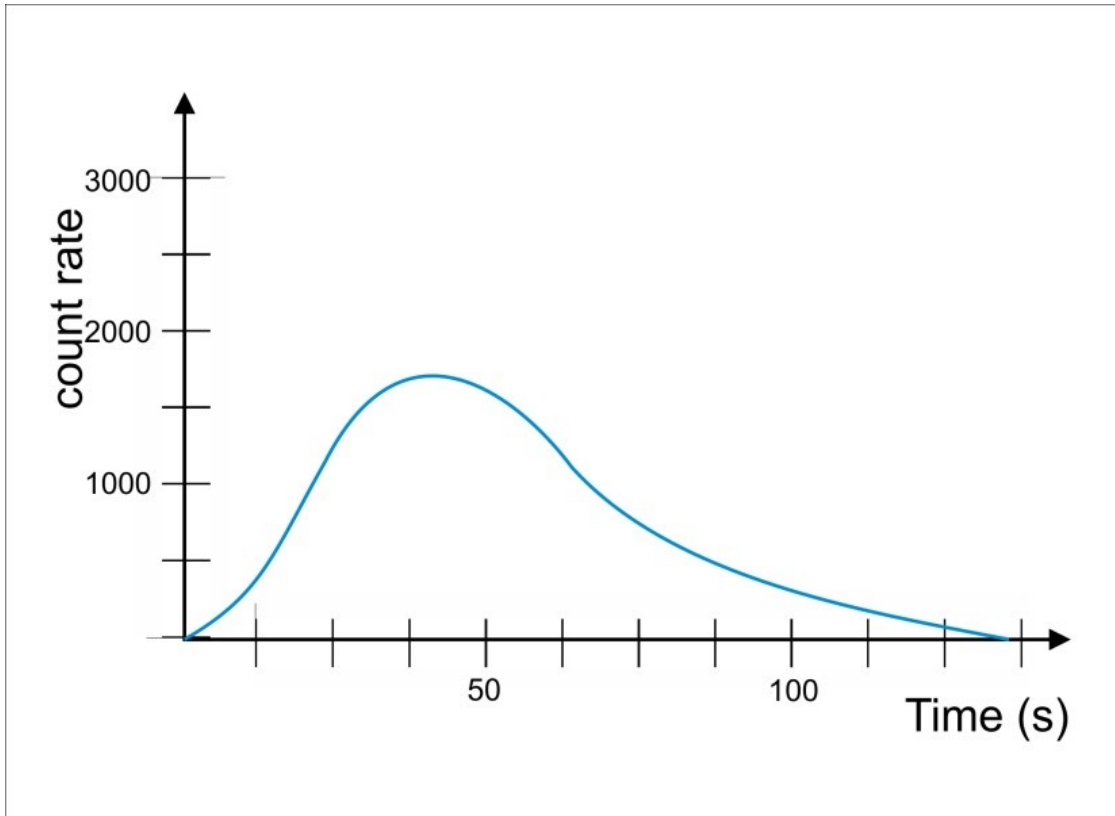


**Figure 2.3:** A plot of tracer concentration at the outlet versus time (IAEA, 2008).

A given volume of the reactor could be inaccessible due to scaling, hardened material or other barriers. This inaccessible volume is referred to as the dead volume and can significantly reduce the performance of the reactor. In such a case, the experimental MRT will be shorter than the theoretical MRT i.e.  $\tau > \tau_a$ , and the dead volume can be determined using the equation (5);

$$V_d = Q(\tau - \tau_a) \quad (2.5)$$

where  $V_d$  is the dead volume.

The standard deviation of the MRT describes the spread of the RTD curve and is an indication of the mixing rate of the medium through the reactor. Figure 2.3 shows RTD curves for different mixing rates. The square of the standard deviation (the variance) is given by equation (6);

$$\sigma^2 = \int_0^{\infty} (t - \tau_a)^2 E(t) dt \quad (2.6)$$

where  $\sigma$  is the standard deviation. It is noted that the standard deviation is greatest when there is perfect mixing in the reactor, and decreases with the degree of mixing.

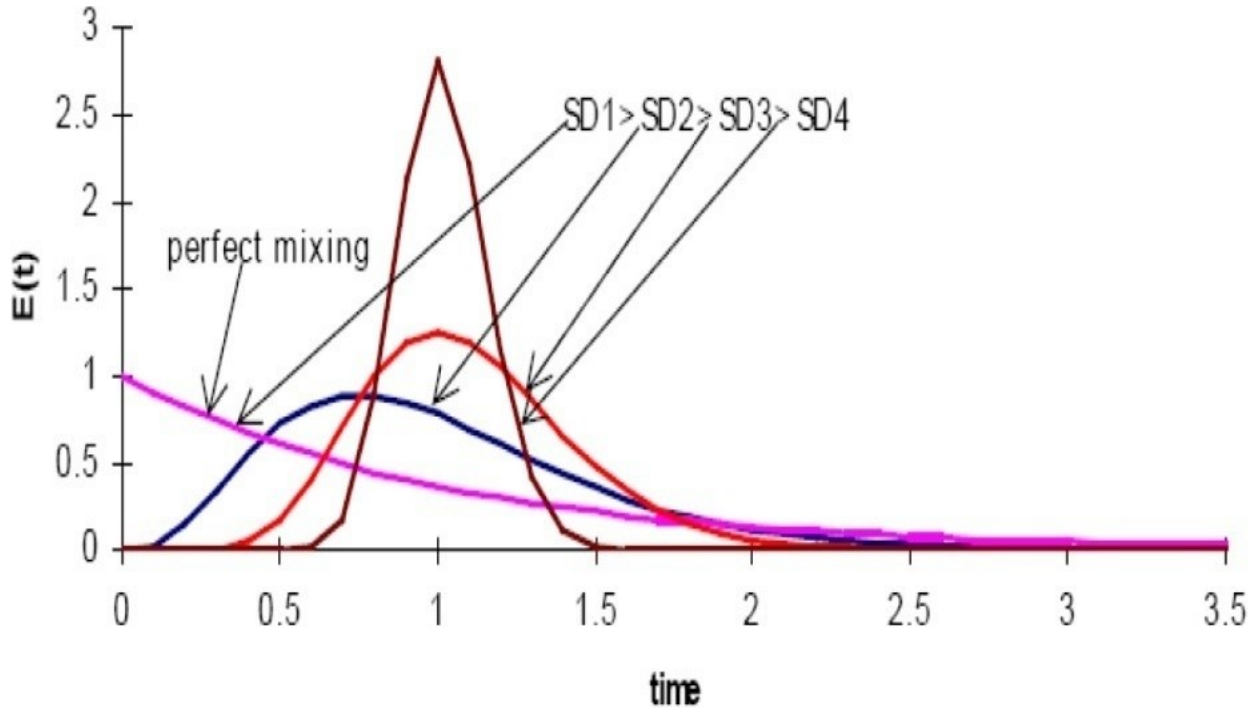


**Figure 2.4: RTD curves with different standard deviations** (IAEA 2008).

To determine the true behaviour of the reactor, mathematical models are used in conjunction with the experimental data. This is achieved using RTD software, where a model is proposed whose resulting RTD curve best fits the experimental curve (Abdelouahed and Reguigui, 2011). The model proposes the configurations of the reactor based on parameters such as type of mixing, type of flow, number of tanks, series or parallel arrangement, and recycling (Kasban et al., 2010). The modelled configuration that produces an RTD curve that reasonably fits the experimental data is chosen as the true behaviour of the reactor. Comparing this behaviour/configuration with the ideal behaviour of the reactor, allows the investigator to diagnose any problems with the reactor.

### 2.3 Selection of Radiotracers for Industrial Applications

Several factors must be considered when selecting the radiotracer to be used. One of the main considerations is the physical and chemical compatibility of the tracer with the material to be traced (IAEA, 2008). In some cases, for example, when studying solubility and chemical kinetics, the tracer is required to be chemically identical to the material being investigated and may be referred to as a chemical radiotracer (IAEA, 2004). There are, however, other studies that do not require the radiotracer to be chemically identical to the

substance being traced. In such cases, the radiotracer is only required to meet a not-so stringent set of physical and physicochemical conditions and may be referred to as a physical radiotracer. The type and energy of radiation must be such that it is easily detected by the chosen method of detection (Loveland et al., 2005). This is in addition to the radiotracer having a long enough half-life and adequate specific activity for the experiment. Finally, the availability and cost of the radiotracer, the type of measurement (whether by sampling or in situ), and radiation safety regulations are also taken into account.

In tracing solid media, the material can be labelled by using either direct activation or surface labelling (IAEA, 2008). In the direct activation technique, a sample of the material under study is exposed to a neutron flux in either a nuclear reactor or a particle accelerator for an appropriate duration. This irradiation results in the production of radioisotopes with the required activity within the material. Table 2.1 lists some of the materials labelled through direct activation

**Table 2.1 Examples of radiotracers induced through neutron activation of solid materials**

Irradiated solids	Induced radioisotopes	Half-life	Radiation type	Radiation energy (MeV)
Clinker	$^{140}\text{La}$	40 hours	Gamma	1.16 (95%) 0.92 (10%) 0.82(27%) 2.54 (4%)
	$^{24}\text{Na}$	15 hours	Gamma	0.55 (70%) 1.32 (27%)
Coal	$^{59}\text{Fe}$	44.5 days	Gamma	1.10 (56%) 1.29 (44%)
			Beta	0.15 (53%) 0.08 (46%)
	$^{46}\text{Sc}$	84 days	Gamma	1.84 (100%) 0.89 (100%)
Copper ore	$^{64}\text{Cu}$	12.7 hours	Gamma	1.35
			Beta	0.19
			Positron	0.28
	$^{42}\text{K}$	12.3 hours	Beta	3.53
	$^{59}\text{Fe}, ^{140}\text{La}, ^{24}\text{Na}$			
Gold ore	$^{198}\text{Au}$	2.7 days	Gamma	0.41 (99%)
	$^{51}\text{Cr}$	28 days	Gamma	0.32 (9.8%)
	$^{56}\text{Mn}$	312.1 days	Gamma	0.84 (100%)
	$^{59}\text{Fe}, ^{42}\text{K}, ^{140}\text{La}, ^{24}\text{Na}, ^{46}\text{Sc}$			

(IAEA, 2008; CNSC, 2017; Yunos, 2016)

The use of direct activation in the production of radiotracers is limited by the availability of nuclear reactors and particle accelerators both of which are not common in the developing world. Surface labelling is an alternative to direct activation through which already existing radioisotopes are used to label the solids. This is achieved through adsorption of the radiotracer onto the surface of the solids by either soaking or sprinkling the solids with the radioactive solution (IAEA, 2008). Examples of radiotracer solutions that are commonly used for surface labelling are listed in Table 2.2

**Table 2.2 Examples of aqueous radiotracer solutions used in surface labelling**

Chemical form	Radioisotope
Chloroauric acid	$^{198}\text{Au}$
Chromium(III) chloride	$^{51}\text{Cr}$
Scandium chloride	$^{46}\text{Sc}$

(IAEA, 2008)

### 2.3 Detectors and Modelling Software

The most preferred detectors in radiotracer RTD studies are scintillation detectors utilizing a single sodium iodide crystal doped with thallium, NaI(Tl). Scintillation detectors offer the advantage of higher detection efficiency of gamma rays when compared to other types of detectors (Knoll, 2010). Among inorganic scintillators, NaI(Tl) is commonly used owing to its commercial availability at low cost and in sizes much larger when compared to alternatives. It also has good light yield and linearity, whereas the high atomic number of iodine ensures a high probability of the photoelectric effect.

The acquired signal must undergo several treatments to give meaningful data. The corrections performed on the experimental curve include; background correction, radioactive decay correction, smoothing to remove statistical fluctuations, extrapolation of the curve and normalization of the area under the curve (IAEA, 2004). Kasban et al., (2010) describe the new trends in RTD signal processing and signal identification. One of the highlights is a novel approach for identifying RTD signals in cases where the background noise is relatively high. The method uses neural networks to identify up to 100% of all signals at all signal-to-noise ratios (SNRs).

The treated RTD data is then modelled to obtain a quantitative description of the flow behaviour of the transported material (IAEA, 2008). The DTS Pro software is one of the programs used for this purpose and incorporates several fluid flow models ( Progepi/Sysmatec, 2000). The software uses the approach proposed by Danckwerts (1953), where the fluid is considered to be a system that can be characterized using its residence time distribution. It can either model the response of a system to a given signal at the inlet or, where the experimental response is available, optimize the parameters of the model so that the calculated response is as close as possible to the experimental response. The software has elementary flow models describing basic fluid flow phenomena, which may be ideal or non-ideal. Models for ideal flows include the plug flow model and the perfect mixer model. Models for non-ideal flows include the axial dispersion model, the perfect mixers-in-series model, and dispersion and exchange models. Different combinations and arrangements of these basic models are used to model a system response close to the measured experimental response. The output is a graphical comparison of the modelled and experimental plots.

The IAEA (2001) has highlighted alternatives to the DTS Pro software that can be used in the modelling of RTD data. One of them is the RTD software developed by the Czech Technical University, CTU; it yields similar results to DTS Pro but was found to be less user-friendly as its interface is based on the Microsoft Disk Operating System (MS-DOS). This is in contrast to DTS pro which uses the more user-friendly windows graphical interface. The CTU software requires the user to input the equations describing the flow models, further compounding its difficulty of use. The commercially available Matrix laboratory (MATLAB) software has also been used to treat, process and model RTD data. It does, however, require the user to be knowledgeable in computer programming.

## **2.4 Review of Studies On Application of Radiotracers in Industry: Residence Time Distribution Method**

P. V. Danckwerts (1953) pioneered residence time distribution studies with his paper on continuous flow systems. He showed how the age distribution of fluid particles through a vessel varied on the type of flow and mixing. In addition, the paper demonstrated how the performance of a reactor can be calculated from its f-diagram – a cumulative residence distribution curve. The paper also describes how the residence time distribution curve of a system can be predicted from a scaled-down model of the system. Charlton (2012) described how radioactive isotopes could be used to conduct residence time measurements in industry and how that resulted in cost savings.

More recently, radiotracer RTD studies have been used to evaluate performance and troubleshoot a wide range of industrial processes. Zahran et al. (2009) used iodine-131 as a tracer to determine the RTD of a phosphate production unit. They used the experimental data generated and subsequent computer modelling to determine whether the unit behaved like perfect mixers in parallel.

Sheoran et al. (2016) carried out radiotracer studies in an industrial-scale paper pulp digester and were able to determine parallel flow channels had formed in one of the tubes. In a more recent study, Sheoran et al. (2020) used radiotracers to determine the optimum operating conditions for a pulp digester. Similar studies have been done on a pilot-scale neutron poison tank by Pant et al. (2015) with the results showing the volume of stagnant fluid in different modes of operation. Adwet et al. (2019) used iodine-131 to evaluate the hydraulic performance of an anaerobic pond at Dandora Waste Water Treatment Plant, Nairobi, Kenya. The study revealed that a huge portion of the pond was a dead volume resulting in a high degree of inefficiency in treating wastewater. The IAEA (2008) also lists fluid catalytic cracking units, trickle bed reactors, mineral floatation tanks and dust cyclones as some of the industrial processes that have been studied using radiotracers.

Globally, RTD measurement is one of the most frequently carried out applications of radiotracers in industrial processes including milling (Plasari et al., 1999; Makokha 2014; Adzaklo et al., 2016; Hassanzadeh, 2018; Vinnett et al., 2018; Abdelouahed et al., 2018; Sheoran et al., 2018, Goswami et al., 2020). Plasari et al. (1999) carried out a radiotracer investigation for the measurement of RTD in a rod mill to develop a model that could predict the product particle size distribution for different material feed rates.

Mumuni et al., 2011 used the radiotracer technique to measure RTD to determine the mean residence times and performance of two clinker grinding ball mills in a cement plant in Ghana Cement (GHACEM). The authors used gold-198 as chloroauric acid ( $\text{H}^{198}\text{AuCl}_4$ ) adsorbed on the solid process material as a radiotracer. The investigation revealed that out of the two mills, one of the mills was operating at a lower efficiency than that expected from the design specifications. About 50% of the process material leaving the outlet of the mill, was above the required fineness and was being recirculated back to the mill inlet. Another study in the same plant suggested that the feed material could be held up for longer in some zones of the mill, resulting in reduced efficiency and thus resulting in higher than expected energy usage (Adzaklo et al., 2016).

As with other industrial unit operations, the efficiency of a ball mill is largely affected by the flow characteristics and residence time of the material inside the mill. Therefore, a mill can be viewed as a reactor whose reaction is to convert large particles into smaller particles (Plasari et al., 1999). The implication is that conventional flow models can be used to describe the flow dynamics of feed material within the ball mill, for example, the perfect mixers-in-series model (Weller, 1980). Adzaklo et al. (2016) in their study of the ball mill at GHACEM found that its flow behaviour was best described by a perfect-mixers-in-series with exchange model. The exchange component resulted in a long tail in the RTD curve, which suggested that the material was taking longer than necessary in the ball mill. Hassanzadeh (2017) conducted a RTD study on a closed circuit ball mill, which revealed that it was operating under over-filled conditions leading to a low breakage rate of the feed. This was accomplished by modelling RTD data which indicated a good fit with a plug flow model combined with two perfect mixers in series. The study was however conducted using sodium chloride as a tracer.

## **2.5 Research Gaps**

The radiotracer RTD investigations carried out by Adzaklo et al (2016) and Mumuni et al (2011) on clinker grinding ball mills utilized gold-198, an isotope that is produced through direct activation in a nuclear reactor (Souza et al., 2022). Makokha et al (2011) and Hassanzadeh (2017) on the other hand used a chemical tracer, sodium chloride, in their RTD assessments of industrial ball mills. There exists, therefore, an opportunity to explore the use of Technetium-99m in RTD studies of ball mills, as it is readily available in Kenya and other developing countries due to its application in medical imaging. Tc-99m emits a lower energy gamma of 140.51 KeV and has a short half-life of 6 hours, this makes it safer for field radiotracer



measurements due to the comparatively lower ionization and reduced time of exposure (IAEA, 2008). Since it is produced by a generator, it can be eluted for several measurements.

## CHAPTER THREE: MATERIALS AND METHODS

### 3.1 Study Location and Facility

The study was undertaken at the National Cement Company Limited plant located on coordinates (1°29'31"S, 37°03'19"E) at the Athi River town, Machakos County, Kenya as shown in Figure 3.1. The National Cement Company Limited plant has a production capacity of 2 million tonnes per year in 2015. It is the second largest producer of cement in Kenya (Oxford Business Group, 2016). The plant produces two different types of cement; Simba Cement 32.5R, Portland Pozzolana Cement (PPC) and Simba Power 42.5R, an Ordinary Portland Cement (OPC). The raw materials used in the manufacture of both types of cement are clinker and gypsum, however, in the manufacture of PPC, pozzolana is also added.

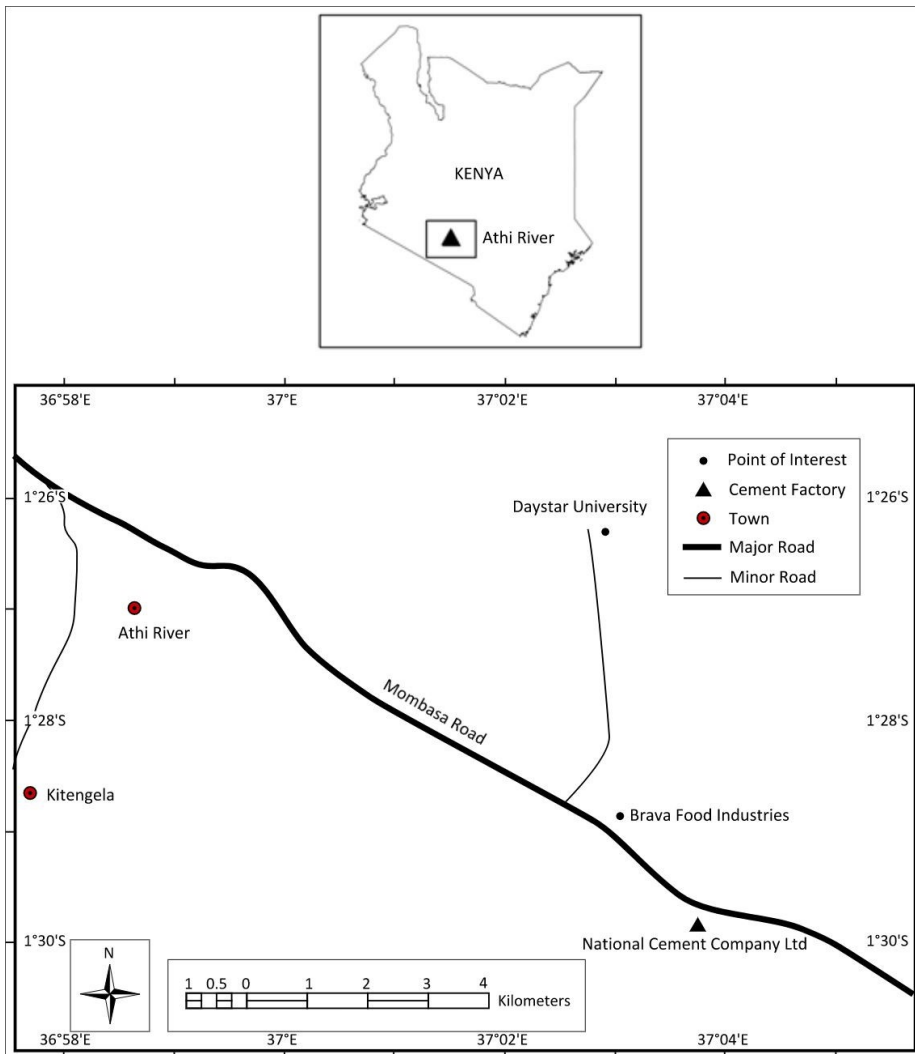


**Figure 3.1: A map showing the location of the NCCL Athi River Plant (1°29'31"S 37°03'19"E).**

In the production of Portland Pozzolana cement, the mill's main product, the raw material composed of 60% clinker, 35% pozzolana and 5% gypsum, was fed into the mill at a rate of 50 tonnes per hour. Additionally,

the mill was set to rotate at 19 rpm and the material was expected to have a residence time of 10 minutes. The product from the mill outlet was fed to a separator, where the coarse particles are separated from the fine particles. After separation, the coarse particles were then returned to the mill inlet for further grinding as shown in Figure 3.4, whereas the finer particles are stored and packaged as cement.

### 3.2 Radiation Safety and Personnel Exposure Monitoring

Adequate radiation safety precaution measures were put in place for use; during transportation, and preparation of the radiotracer for use during the measurements in this study.

The Tc-99m generator, by design, had an external casing and a built-in lead shield for protection against radiation. The generator was transported to and from the plant in the boot compartment of the transport vehicle, and radioactivity was monitored continuously, using a radiation survey meter. The results of the radiation monitoring are shown in table 3.1. The study area at the plant was cordoned off for access during measurements, except only for the assistants present, at the milling plant during the duration of the measurements. Lead shields were used to cover both the vial carrying the eluted radiotracer solution and the syringe used to draw the solution.

**Table 3.1: Radiation doses recorded in the vicinity of the Tc-99m generator**

Distance from generator (cm)	Recorded dose ( $\mu\text{Sv}$ )
30	16.7
1000	4.5

All personnel were routinely monitored for radiation exposure throughout using Rados Rad-60 personal dosimeters, following prior authorization from the Kenya Nuclear Regulatory Authority (KNRA). The materials leaving the mill were monitored for residual radioactivity contamination. The effective dose received by the author and the research assistants is tabulated in table 3.2. This is the total dose received in the 14 hours spanning loading of the generator onto the vehicle, transportation of the generator to the cement plant, execution of the radiotracer study, transportation of the generator back to the institute and offloading of the generator. The recorded values were well below the annual dose limit of 20 millisieverts for radiation workers (ICRP, 2007).

**Table 3.2: Total Effective dose received in the duration of the investigation**

Personnel	Effective dose ( $\mu\text{Sv}$ )
Principal researcher	56
Research assistant 1	49
Research assistant 2	52

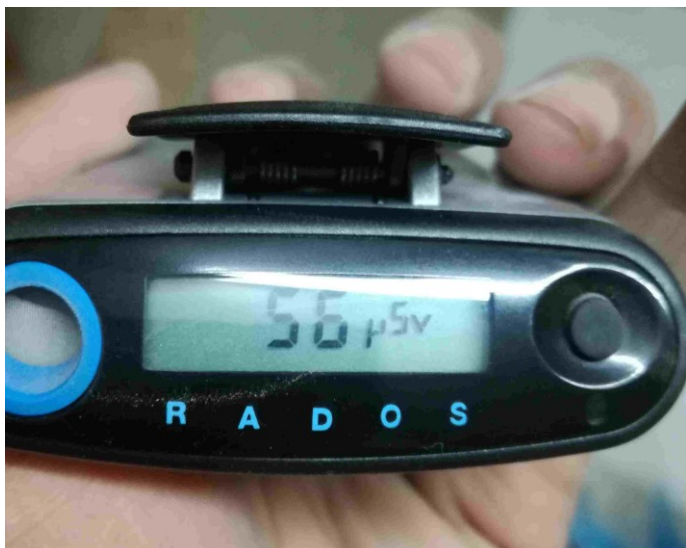


**Figure 3.2: The dosimeter used by the author, showing the effective dose at the end of the investigation**

### **3.3 Radiotracer measurements: Materials and Instrumentation**

#### **3.3.1 Instrumentation**

The radiotracer detector assembly used in this study consists of the following; Scintillation Crystal: NaI(Tl) (1.5'' x 2''), with a resolution of 7.3% at 662 keV, operating at Gamma energy range: 25 to 2500 Kev; and at temperature range: -5<sup>0</sup>C - 85<sup>0</sup>C, with 10 stage multiplier tube assembly and 50 m BR2-BR2 cable on a roll. The detector efficiency was checked using a 370 MBq Strontium-90 source and found to be adequate for the field investigation. The Altaix Data Acquisition System used, consisted of a 12-channel data acquisition module that utilizes software designed for radiotracers and nucleonic control functions (Fig. 3.2, 3.3).

The following was the data acquisition sequence:

- a) Selection of parameters: tracer type and preparations, sampling time, duration of the experiment (choosing the right time to stop data acquisition);
- b) Data Acquisition and treatment;
- c) Modelling for system analysis.



(a)

(b)

**Figure 3.3: Thallium-activated sodium iodide detectors (a) and Connecting cable 50m long (b)**



**Figure 3.4: Laptop placed on top of the Altaix Data Acquisition System**

### 3.3.2 Radiotracer Material and Preparations

Technetium-99m was the radioactive tracer used for the measurements, it is produced in a generator from the decay of molybdenum-99. Tc-99m has a half-life of 6 hours, it emits gamma radiation with an energy of

140.51 keV (100%) and is available as sodium pertechnetate aqueous solution. The half-value layer for Tc-99m is 8.1 mm for steel, and the gamma-ray emission can thus penetrate a single wall thickness of 10 mm thick steel pipe at the inlet and outlet of the ball mill, for online monitoring (Canadian Nuclear Safety Commission, 2017). The expected residence time of process material in the ball mill was estimated to be about 10 minutes, which was significantly less than the half-life of Tc-99m.

The brand of the Tc-99m generator used was NovaTec-P, supplied by NTP Radioisotopes, South Africa via their subsidiary AEC-Amersham SOC Ltd, South Africa. The parent radionuclide, Mo-99, was adsorbed on an alumina column inside the generator. To elute the Tc-99m, an evacuated collection vial was first inserted at the outlet followed by the introduction of a saline solution at the inlet as shown in figure 3.4. The eluate containing the tracer then flowed into the collection vial as a result of the pressure differential.

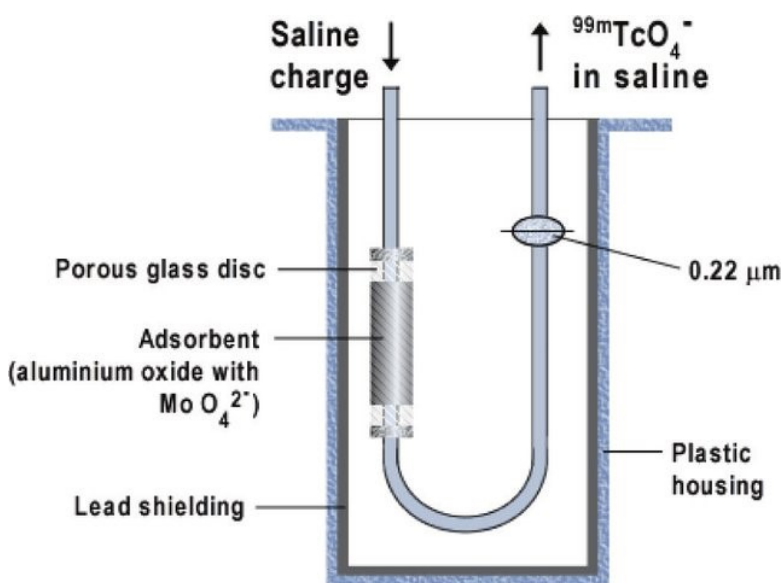


**Figure 3.5: Schematic diagram of a typical technetium-99m generator (Hidayati, 2016)**

The generator had been pre-calibrated by the supplier to produce a Tc-99m solution with an activity of 2000 MBq (54 millicuries) at the time of the first elution. The radiotracer was prepared by labelling the porous clinkers with this radiotracer solution. About 250 g of clinker material from the outlet of the rotary kiln was collected, mixed in 400 ml of the Tc-99m aqueous solution, and stirred for 40 minutes. Subsequently, the clinker nodules were dried on a hot plate for 10 minutes. Based on the radiotracer concentration in the initial solution, the activity of the prepared radiotracer was calculated to be about 1782 MBq, for the first run, at the time of injection into the system (10 minutes after the drying process). The same procedure was repeated for the second run, however, the activity of the Tc-99m solution was lower at 660 MBq since it was eluted two hours after the first run. After mixing with the clinker, the resulting radiotracer for the second run had an activity of 588 MBq.

### 3.3.3 Field Radiotracer RTD Measurements

The radiotracer investigation was undertaken on mill 1, the oldest of three clinker grinding ball mills at the plant.

The Tc-99m labelled clinker tracer was instantaneously injected at the inlet of the ball mill, as shown in figure 3.4, and monitored at three locations i.e., inlet and outlet (D1, and D2) of the mill and as well as at the recycle line(D3), using three independent NaI(Tl) scintillation detectors connected to a computer-controlled ALTAIX data acquisition system (DAS). The data acquisition system was set to record radiotracer concentration (counts/unit time) every second until the radiation intensity at three locations was reduced to the natural background levels. The mean natural background radiation levels were monitored before injection of the tracer and found to be 22, 79 and 18 counts per second for detectors D1, D2 and D3 respectively. Two repeat radiotracer measurements were done to compare the curves obtained at different radiotracer activity levels. Figure 3.5 shows the conveyor at the inlet of the ball mill. Figure 3.7 shows the interior of the clinker ball mill and Figure 3.8 shows the location of the Detector D3 at the recycle line from the separator.

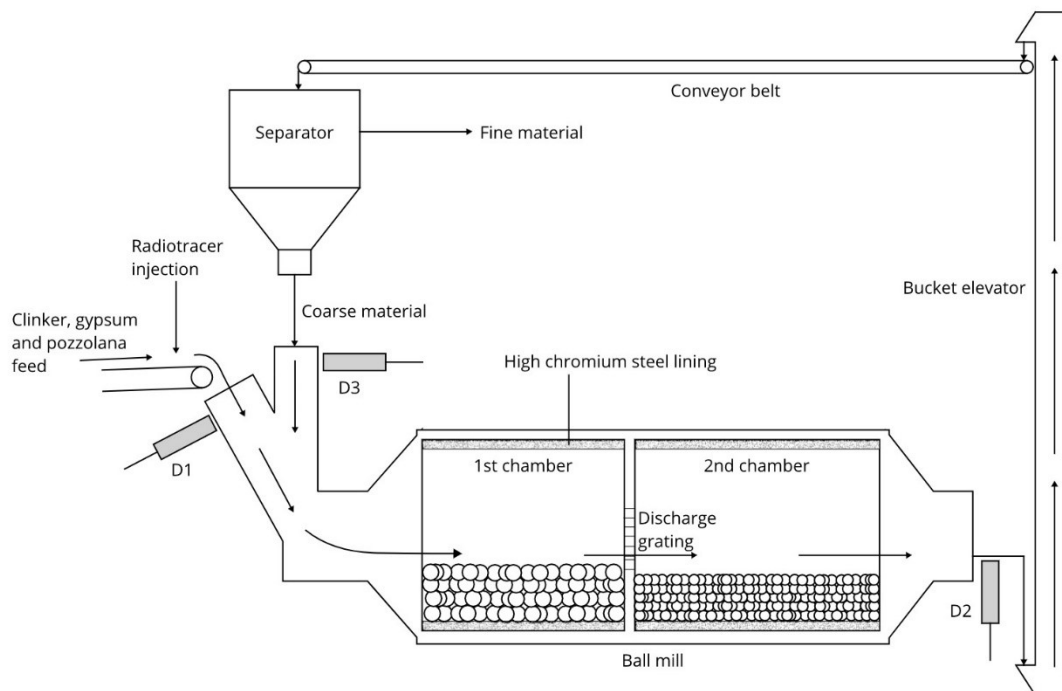


Figure 3.6: Ball mill in closed circuit mode {D1, D2 and D3 are detectors (Mumuni et al., 2011)}.



**Figure 3.7: The point of introduction of the tracer - the conveyor at the inlet of the ball mill**



**Figure 3.8: The interior of the second chamber of the clinker ball mill**





**Figure 3.9: Detector D3 with a lead collimator at the recycle line from the separator**

### **3.3.4 Data Treatment and Analyses**

The radiotracer concentration curves were plotted for three different locations in the ball mill, they were corrected for natural background levels, time zero shift, smoothing and tail correction.

The plots of radiotracer concentration recorded at the outlet of the mill (D2) and at the inlet of the separator in the recycle line (D3) were shifted toward zero by a time equivalent to the time of occurrence of the Delta pulse. After background correction and zero-shift, the data (D2 and D3) were smoothed using a repeated average method i.e. by increasing the sampling time from 1 second to 10 seconds. The data recorded by detectors D2 and D3 had a long tail that was infested with large fluctuations and was thus corrected using the exponential decay method (IAEA, 2008). The fluctuations can be attributed to the low signal-to-noise ratio in the tail where the activity of the tracer was lowest. The logarithm of the measured count rates was first plotted against time, this resulted in a linear plot which confirmed that the activity was decreasing exponentially. The logarithmic function of this plot was then used to extend the curve to the point where the tracer activity was zero. The time of RTD measurements was much shorter than the half-life (6 h) of the radiotracer and thus no decay correction was required to be applied to the data.

### **3.4 Flow model Simulation: DTS PRO software**

The RTD data obtained, during the measurements, was modelled to infer the behaviour of the system, using DTS PRO software developed by PROGEPI. The software contains 8 elementary flow models and describes the procedures, on how they can be combined, to give a model response similar to the experimental response ( PROGEPI/SYSMATEC, 2000). Various combinations of these elementary models are used to describe complex processes and their fluid dynamics.

The flow models integrated into the software are categorized into two types; plug flow reactor models and perfect mixing models. Perfect mixing models include; perfect mixer, perfect mixers in series, perfect mixers in series with dead volume, and perfect mixers in series with back-mixing whereas, plug flow models include; simple plug flow, plug flow with axial dispersion open to diffusion, plug flow with axial dispersion half open to diffusion and plug flow with axial dispersion closed to diffusion. These models are conceptualized in figures 3.10 and 3.11, respectively.

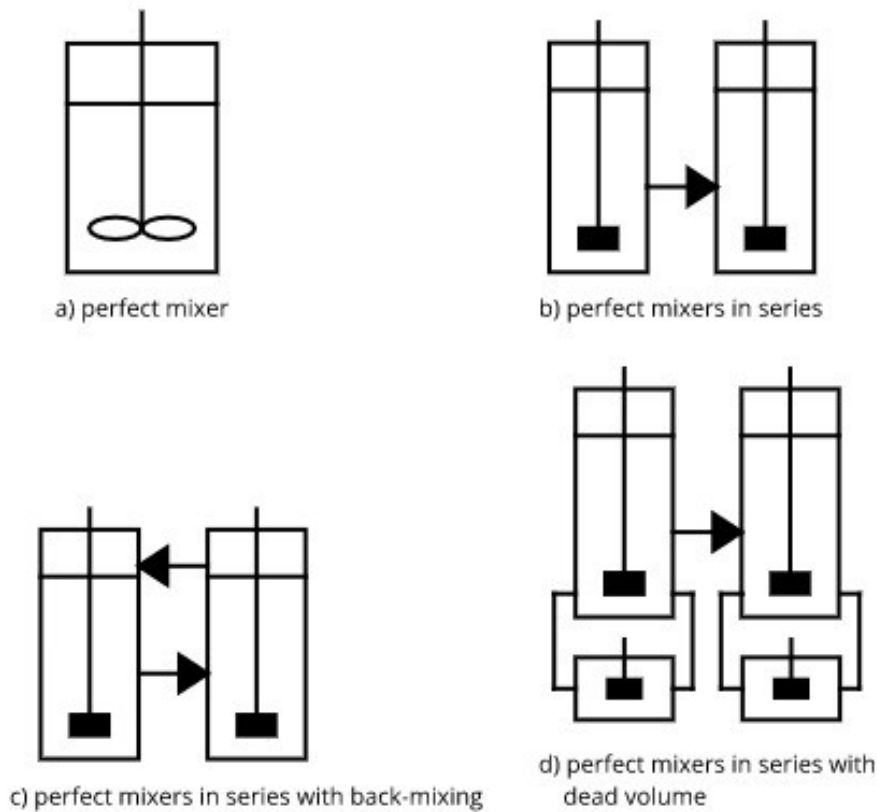


Figure 3.10: Perfect mixing models ( PROGEPI/SYSMATEC, 2000)

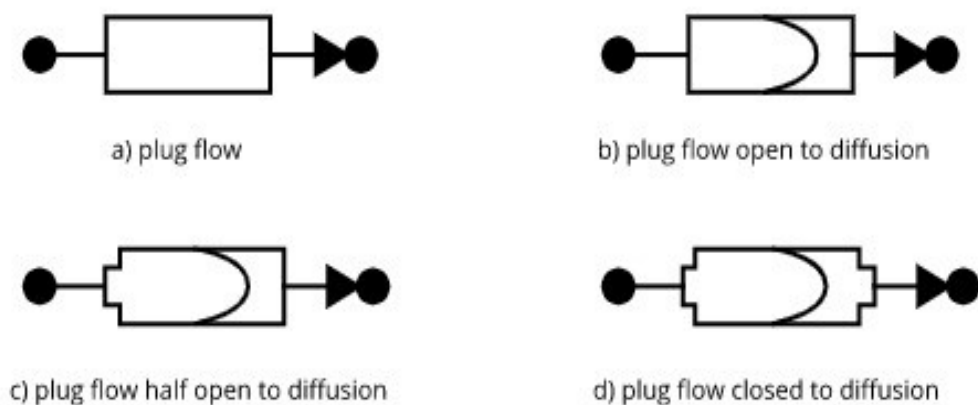


Figure 3.11: Plug flow models ( PROGEPI/SYSMATEC, 2000)

### 3.4.1 Perfect Mixer

This model assumes ideal mixing leading to homogeneity, where concentrations are uniform across the entire reactor vessel. In this scenario, two parameters are taken into account in the software i.e. the mean residence time ( $\tau$ ) and the volume ( $V$ ). Either one of these can be varied by the user during the modelling, but not both at the same time. In this study,  $\tau$  was varied.

### 3.4.2 Perfect Mixers in Series

Here reactor flow was modelled as being through two or more perfect mixers, where the output of the first is the input of the second and so on. Three parameters are taken into account i.e. the mean residence time ( $\tau$ ), the volume ( $V$ ), and the number of mixing tanks ( $J$ ).

### 3.4.3 Perfect Mixers in Series with Back-mixing

This model is similar to the perfect mixers in series in the arrangement of tanks, however, a portion of the material is assumed to flow back, in the opposite direction to the normal flow of the process in the reactor vessel. In this case, there are four parameters considered for variation, namely; mean residence time ( $\tau$ ), the volume ( $V$ ), the number of mixing tanks ( $J$ ) and the proportion of the flow rate that is back-mixing ( $\alpha$ ).

### 3.4.4 Perfect Mixers in Series with a Dead Volume

In this model, the reactor vessel is assumed to have, in addition to the perfect mixers, a stagnant zone also referred to as a dead volume as indicated in Figure 3.10. The dead volume is conceptualized as another mixer with volume  $V_2$  that exchanges some material with each perfect mixer. As a result, the model has seven parameters: the mean residence time ( $\tau$ ), the volume of one of the perfect mixing tanks ( $V_1$ ), the volume of the corresponding dead volume ( $V_2$ ), the number of mixing tanks ( $J$ ) and the fraction of the flow rate of the material moving to and from the stagnant volume ( $\beta$ ), the exchange time constant ( $t_m$ ) and the volume ratio ( $K$ ). The exchange time constant and the volume ratio are calculated as below:

$$t_m = \frac{V_2}{\beta Q} \quad (3.1)$$

$$K = \frac{V_2}{V_1} \quad (3.2)$$

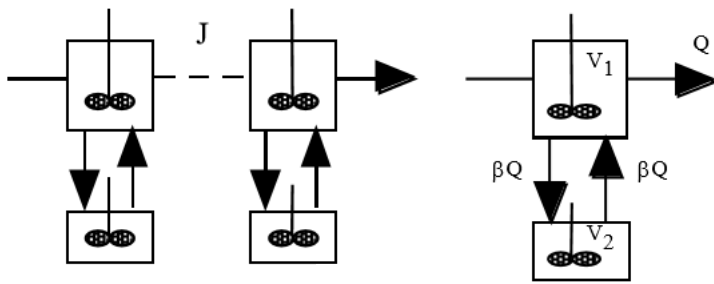


Figure 3.12: Perfect mixers in series with dead volume ( Progepi/Sysmatec, 2000).

### 3.4.5 Plug flow model

In the plug flow model, the material flows in parallel sections without any exchange of material between the sections. All the plug flow models are defined by two parameters namely, the mean residence time ( $\tau$ ) and the Peclet number ( $Pe$ ). The Peclet number is a non-dimensional parameter that indicates the ratio of convective to dispersive effects (IAEA, 2008).

$$Pe = \frac{uL}{D} \quad (3.2)$$

Where  $u$  is the fluid velocity,  $L$  is the length of the system and  $D$  is the axial dispersion coefficient.

### 3.4.5 Plug flow open to diffusion model

This model is also referred to as the axially dispersed model (ADM). It characterizes flow in a plug flow reactor where there is some degree of back-mixing. The response of the ADM for an impulse injection of the tracer at the inlet of the tank for open-open boundary conditions is described as follows (Levenspiel, 1972):

$$E_m(t, p) = \frac{Pe}{\sqrt{4\pi\tau_1 t}} \exp \left[ -\frac{Pe(\tau_1 - t)}{4\tau_1 t} \right] \quad (3.3)$$

Where,  $E_m(t)$ : Impulse response of the model,  $Pe$ : Peclet number,  $\tau_1$ : mean residence time in axially dispersed flow component,  $t$ : time variable.

### 3.4.6 Practical DTS Pro software Modelling

To carry out modelling on the DTS Pro software, the inlet signal had to be specified first; this meant either selecting a Dirac pulse or, in the case where the inlet signal was not a Dirac pulse, inputting the data values observed at the inlet in counts per second (cps). Next, the observed data values, also in counts per second, at the outlet were entered. Based on the technical design and specifications of the reactor system being investigated, one of the models described in the preceding section, or a combination thereof, was selected and the initial values for model parameters were entered.

Once the calculation had been run successfully during the simulation, the plot was visualized for a more precise model that best describes the flow behaviour of the media within the ball mill. The software used the least squares curve-fitting method to fit the experimental and model predicted RTD plots. The quality of the fit was evaluated by selecting the model parameters to minimize the sum of the squares of the differences between the data ( $Y(t)$ ) and model ( $Y_m(t)$ ), identified as the root mean square (RMS) value. The values of the model resulting in the minimum RMS value were selected as the best set of parameters (Michelsen, 1972).

$$RMS = \sqrt{\frac{1}{N_p} \sum_{i=1}^{N_p} [Y_m(t, p) - Y(t)]^2} \quad (3.4)$$

The DTS PRO software provides a graphical environment, where the models earlier described were combined to model the system response. The environment is in the form of a grid with points on which various elements of the model were placed as shown in Figure 3.13. The elements include modules, nodes and connectors. Modules consist of the basic flow models which are represented by a unique symbol for each flow model. The nodes and connectors, on the other hand, provide a means of connecting the modules. To begin with, a module in the toolbox was selected and placed on the grid by clicking once using the left mouse button. The parameter values of the module were then entered by double-clicking it using the left mouse button and entering values in the dialogue box that opened.

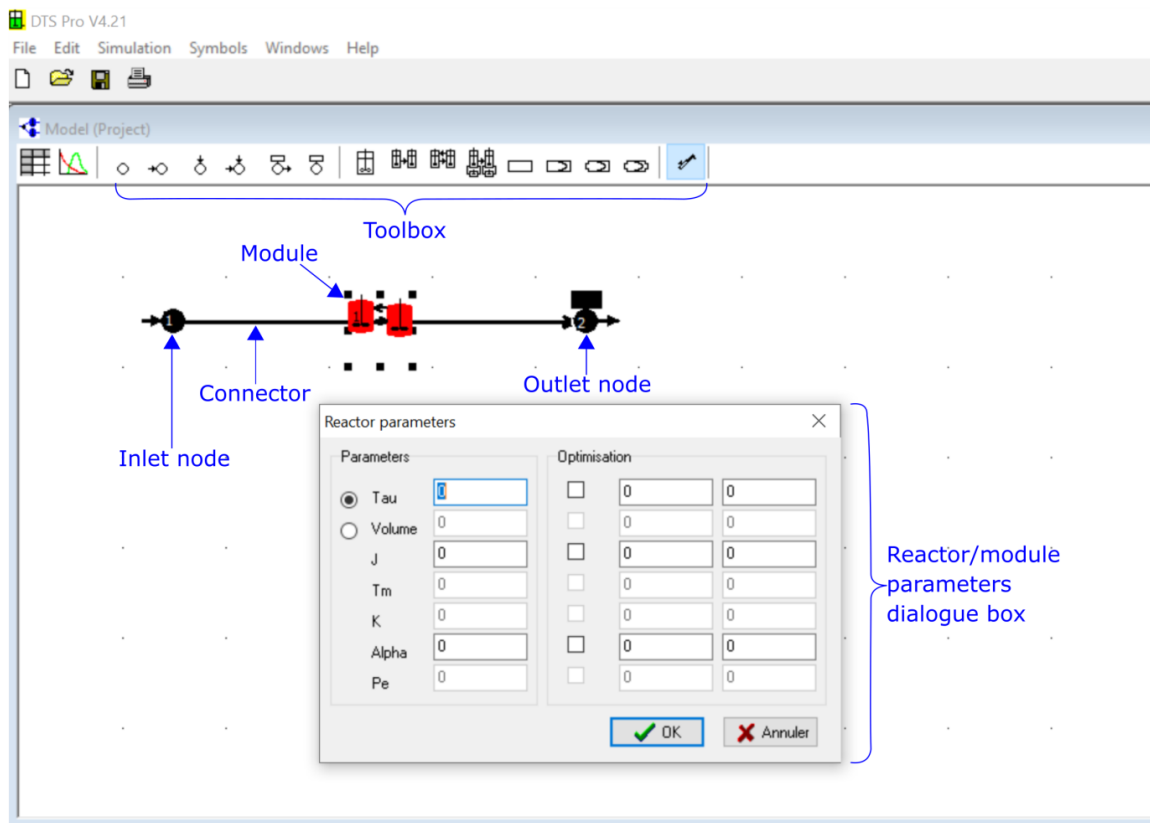


Figure 3.13: The DTS Pro software user interface

Next, the nodes were placed and all the elements were connected using the connectors; it is important to note that the connectors could only begin and end at the nodes. Additionally, the flow-rate parameter value of the connector had to be entered by double-clicking on it.

After building the model, the simulation was run to generate, as an output, the residence time distribution curve of the model. This curve was compared to the experimental curve to determine if it was a good fit. These steps were repeated for several iterations until finally the model giving the curve with the best fit was chosen as the true behaviour of the system under study.

## CHAPTER FOUR: RESULTS AND DISCUSSION

### 4.1 Introduction

In this study, the MRT of the media within the mill was determined to be 980.5 seconds, whereas the clinker holdup was estimated to be 13.6 tonnes within the ball mill. The MRTs of the clinkers within the separator and the entire milling circuit were found to be 44.5 s and 1025 s, respectively. The flow of clinker in the ball mill was suitably described by two models; one, as a plug flow component combined with an axial dispersion component, and two, as a plug flow component combined with a tank-in-series with a back-mixing component.

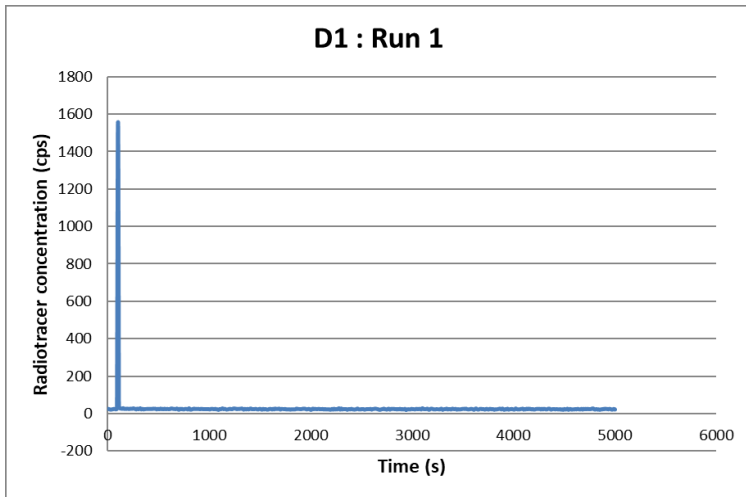
### 4.2 Results of RTD and MRT Measurements

Detector D1 and D3, which were located at the inlet of the ball mill, and at the outlet of the separator, respectively, all recorded a Dirac Delta pulse in both runs, which indicates, that the entire tracer was introduced and recorded, instantaneously. The implication was that no dispersion happened during injection, and any observed dispersion at the outlet would be due to the feed dynamics in the ball mill. D3 recorded the pulse due to its proximity to the inlet of the ball mill. The time of occurrence of the Dirac pulse was considered to be zero, coinciding with the time of injection of the radiotracer into the ball mill. The radiotracer concentration curves observed for D2 and D3 in the second run (figure 4.2) had higher fluctuations when compared to the first run (figure 4.1). This resulted from the decreased activity of Tc-99m used in run 2, 588 MBq in run 2 versus 1782 MBq in run 1. It meant that the detected activity was closer to the background radiation level, and therefore more susceptible to noise interference. Overall, the radiotracer concentration recorded by D3 was significantly lower than that detected by D2 as shown in Table 4.1. This implies that only a small portion of the feed, about 14%, was recycled back into the ball mill for grinding.

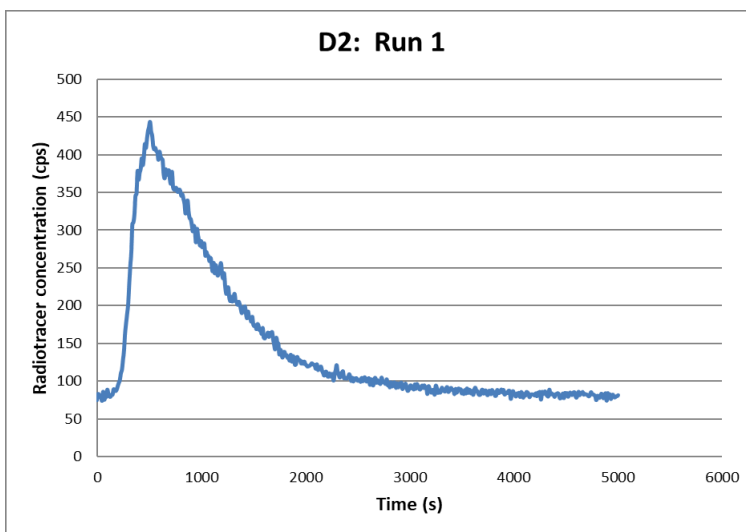
**Table 4.1: Total counts recorded at the ball mill outlet vs total counts at the recycle outlet of the separator**

Detector	Position	Total counts (after removal of background)
D2	Ball mill outlet	349,203
D3	Recycle outlet of the separator	48,784
		Material recycled = 13.97%

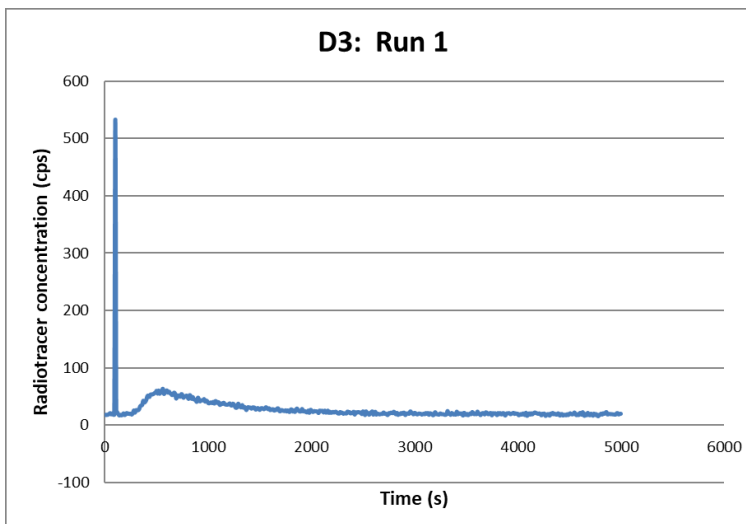
Figure 4.1 (a), (b), and (c) show the changes in radiotracer concentration for each of the detectors D1, D2 and D3, during the first run, while Figure 4.2 (a), (b), and (c) shows the radiotracer concentrations at the D1, D2 and D3 for the second run.



(a)



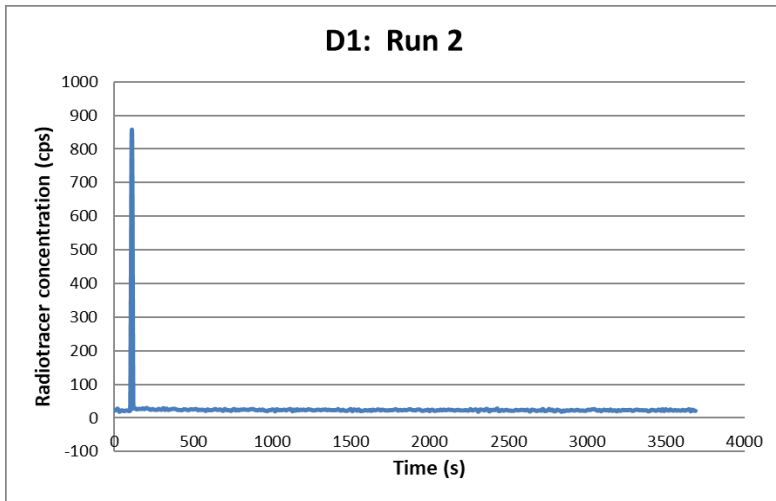
(b)



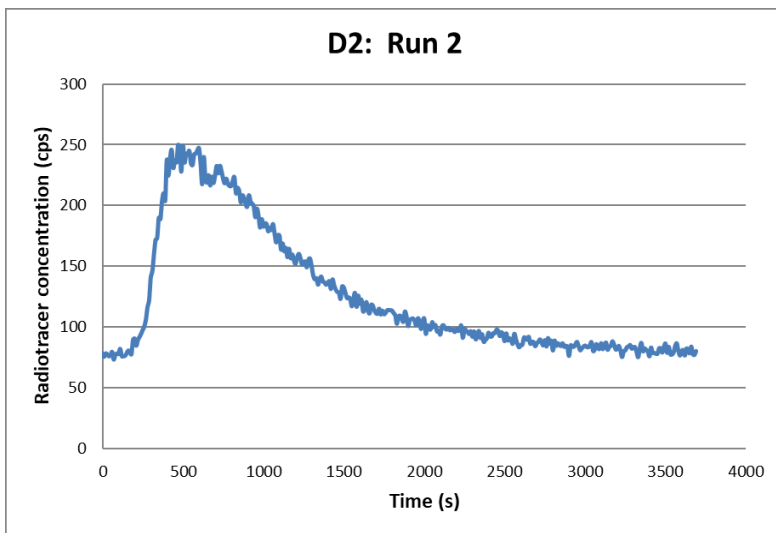
(c)

**Figure 4.1(a), (b), (c): uncorrected radiotracer concentration curves from the 1<sup>st</sup> run for detectors; D1, D2 and D3**

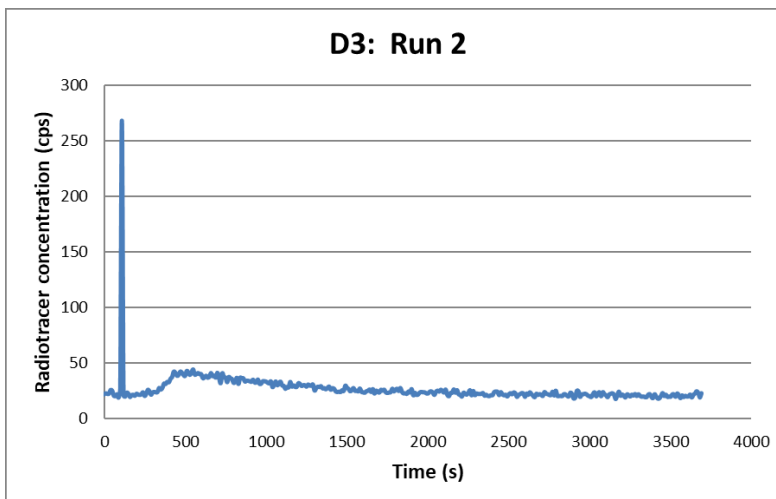




(a)



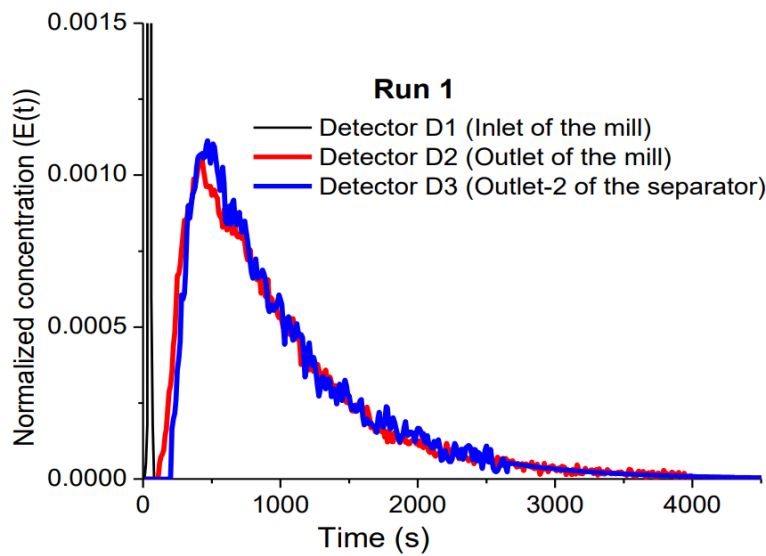
(b)



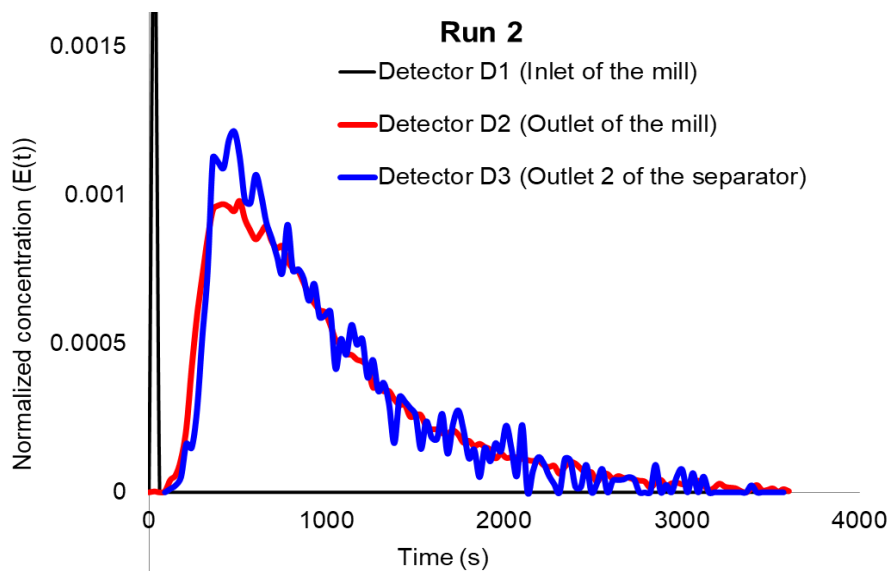
(c)

**Figure 4.2(a), (b), (c): uncorrected radiotracer concentration curves from the 2<sup>nd</sup> run for detectors D1, D2 and D3**

The radiotracer concentration plots recorded at the outlet of the mill (D2) and at the inlet of the separator in the recycle line (D3) were corrected for zero shift by a time equivalent to the time of occurrence of the Dirac pulse. The detectors' response was corrected for background, and data was smoothed for responses at D2 and D3, using a repeated average method by increasing the sampling time, from 1 s to 10 s and corrected for exponential decays (IAEA, 2008). The plots of radiotracer concentration were then normalized by dividing each data point by the area under the tracer concentration curve i.e. the total number of counts recorded. A benefit of normalization is that the curves could be compared without taking into account their areas. The corrected and normalized data for the two runs was plotted as illustrated in figure 4.3.



(a)



(b)

**Figure 4.3: Variations of corrected and normalized radiotracer concentration responses at D1, D2, and D3 for the 1st run (a), and the 2nd run (b).**

The first moments of the curves measured by detector D2 and D3 were calculated using equation 2.4. The first moment of the curve observed at the outlet (D2) of the mill provides the MRT of the media within the mill and was determined to be 978 s and 983 s, for run 1 and run 2 respectively. Similarly, the first moment of the curve recorded by the detector D3 at the recycle outlet of the separator provides the total MRT or mean recycle time of the media within the entire milling circuit, and the same was determined to be 1,000 seconds for run 1 and 1,050 seconds for run 2. The average MRT of the feed in the ball mill was therefore 980.5 seconds, while that for the entire milling circuit was 1,025 seconds.

The difference of the moments of curves measured by detectors D2 and D3 gives the mean residence time of the coarser media within the separator flow circuit, i.e. 22 seconds and 67 seconds for runs 1 and 2 respectively. The difference between the first moments of the curves observed at the outlet of the mill (D2) and the bottom outlet of the separator (D3) provides the MRT of the clinkers within the elevator (vertical conveyer) and the separator, and was determined to be 22 seconds and 67 seconds for runs 1 and 2 respectively. The average MRT of the feed in the elevator and separator was thus 44.5 seconds.

Since MRT is experimentally determined and the feed rate (Q) is known, the holdup (H) of clinkers can be computed by multiplying the two parameters. Table 4.1 shows the summary of the results of MRT measurements.

**Table 4.2: Experimental MRTs and hold-up**

Run No.	Detector No.	$\bar{t}$ (s)	H (tonnes)
1	D2	978	13.6
	D3	1000	13.8
2	D2	983	13.6
	D3	1050	14.6

$\bar{t}$ : experimental mean residence time,  
H: material hold-up in the mill

### 4.3 Flow model Simulation: DTS PRO software

To describe the flow of clinker within the mill and separator, different models and their combinations were used to simulate the recorded radiotracer concentration curves (D2 and D3). A combination of a plug flow component with a tank in series component was modelled, similar to the model proposed by Rogers and Austin (1984), but the curve was found to vary significantly from the experimental curve. Eventually, two models were found to fit very well the observed curves. Figure 4.4 and Figure 4.5 shows the type of models used to visualise the feed dynamics in the clinker mill

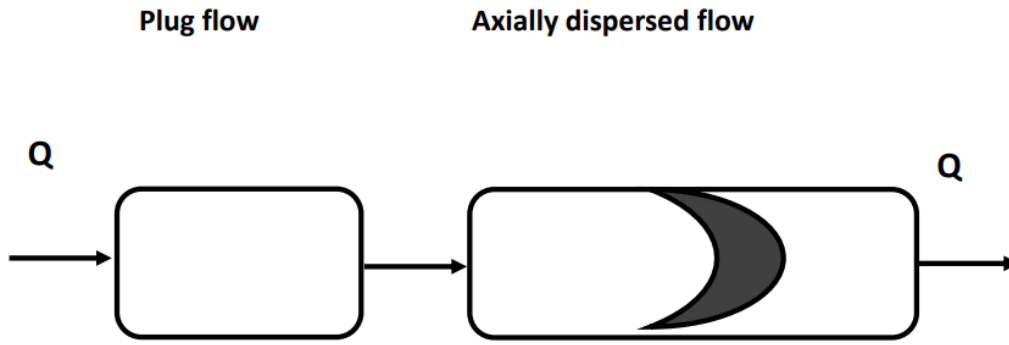


Figure 4.4: Block diagram of Model-1

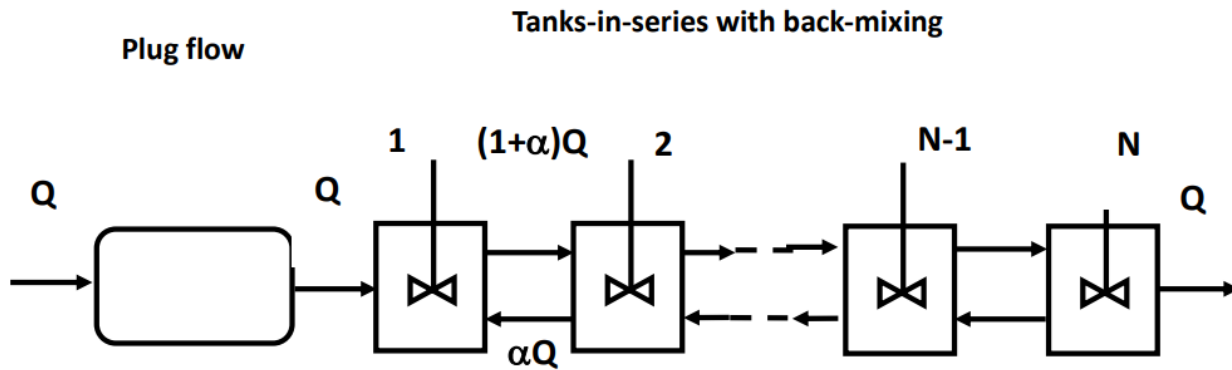


Figure 4.5: Block diagram of Model-2

The Model-1 consists of a plug flow component connected in series with an axial dispersion model (ADM). The response of the ADM for an impulse injection of the tracer at the inlet of the tank for open-open boundary conditions was described by Levenspiel (1972) and more recently by Huang and Seinfeld (2019)

The Model-2 consists of a plug flow component connected in series with a tanks-in-series with back-mixing model. The tracer balance equations and solution of the tanks-in-series with back-mixing model are discussed in detail by Pant et al. (2015).

The comparisons of experimental and model simulated curves are illustrated in Figure 4.6 and Figure 4.7. The values of the model resulting in the minimum RMS value were selected as the best set of parameters. The values of the optimized model parameters that give the best fit are given in Table 4.3.

In Model-1, the plug flow component provides only time-shift to the flow, whereas the ADM model provides axial dispersion (back-mixing) as well as a time delay to the flow. The time delay corresponding to the plug flow segment was found to be about 110 s in the ball mill. The axial dispersion or the back-mixing is quantified in terms of model parameter  $Pe$  ( $UL/D$ , where  $U$ : transport velocity,  $L$ : distance between the two monitoring locations and  $D$ : axial dispersion coefficient). The high value of  $Pe$  implies low axial dispersion or low back-mixing of flow. The low values of  $Pe$  (1.11-1.13) corresponding to minimum RMS obtained after simulations, indicated a high rate of back-mixing of clinkers within the mill.

In the case of simulation of the radiotracer curve observed at the outlet of the mill (D2) using Model-2, similar results were obtained. The low value of the number of tanks parameter,  $N = 3$ , and high back-mixing ratio,  $\alpha > 1$ , also indicated a high degree of back-mixing of clinkers. Similar results were obtained when the curve observed at the bottom outlet of the separator (D3) was simulated. The results also indicated that there was no back-mixing of clinkers within the elevator, conveyor and separator and, the clinkers flowed as a plug flow between the outlet of the mill to the bottom of the separator. This indicated that whatever axial dispersion occurred, it occurred within the mill and there was absolutely no dispersion of the particles within the elevator and the separator.

**Table 4.3: A comparison of the experimental RTD measurements and the flow modelling results**

Run No.	Detector No.	$\bar{t}$ (s)	H (tonnes)	$\tau_p$ (s)	Axial dispersion model (Model-1)			Tank-in-series with back-mixing model (Model-2)			
					$\tau_{ad}$ (s)	Pe	$\tau_1$ (s)	$\tau_{bm}$ (s)	N	$\alpha$	$\tau_2$ (s)
1	D2	978	13.6	100	890	1.11	990	858	3	1.43	958
	D3	1000	13.8	160	840	1.13	1000	825	3	1.4	985
2	D2	983	13.6	120	890	1.1	1100	870	3	1.5	990
	D3	1050	14.6	180	843	1.1	1023	920	3	3	1100

$\bar{t}$ : Experimental MRT, H: Hold-up,  $\tau_p$ : MRT in plug flow component,  $\tau_{ad}$ : MRT in axially dispersed flow component, Pe: Peclet number,  $\tau_1$ : Overall MRT predicted by Model-1,  $\tau_{bm}$ : MRT in back-mixed flow component, N: Tank number,  $\alpha$ : Back-mixing ratio,  $\tau_2$ : Overall MRT predicted by Model-2

The studies carried out by Rogers and Austin (1984) showed that the flow of material in ball mills can be best described by a model consisting of a plug flow component combined with a series of tanks. Adzaklo et al. (2016) also found that the flow of clinker in a ball mill fitted well with a tank-in-series model. Similar results were observed in the present investigation with an exception of back-mixing between the tanks. It can therefore be inferred that the back-mixing observed is a deviation from the expected flow, implying that the feed material spent a longer time than necessary in the ball mill leading to process inefficiency. The mathematical modelling did not indicate the presence of other flow irregularities such as bypassing and dead volume. If present, a dead volume would have been indicated by a tanks-in-series with exchange model whereas the presence of two peaks in the RTD curve would have indicated a bypass in the ball mill volume.

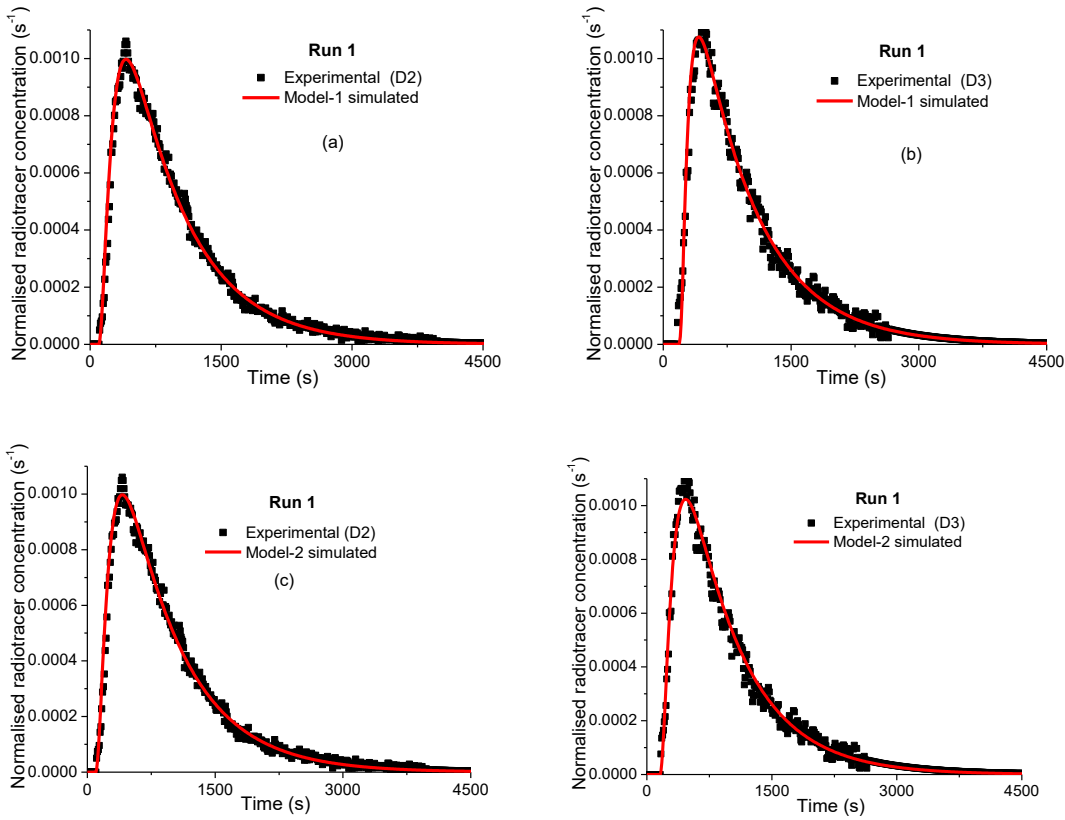


**Figure 4.6: Comparison of experimental and model simulated RTD curves (Run 1)**

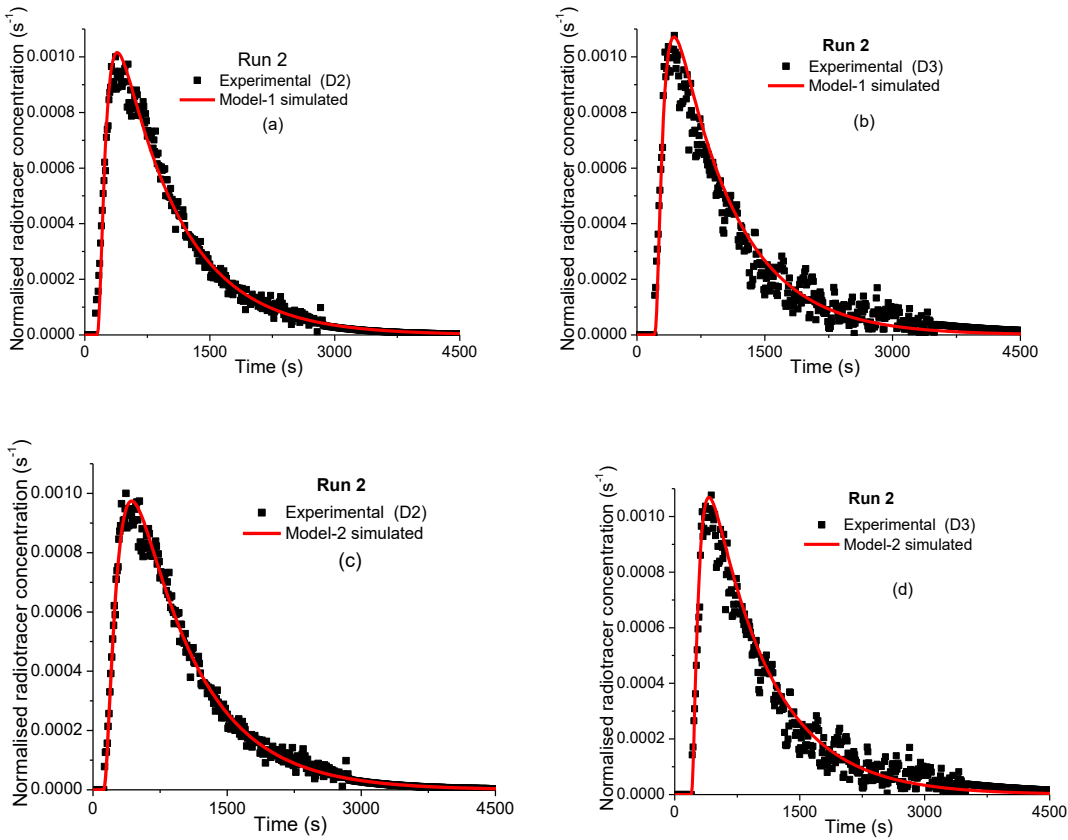


**Figure 4.7: Comparison of experimental and model simulated RTD curves (Run 2)**

## CHAPTER FIVE: CONCLUSIONS AND RECOMMENDATIONS

### 5.1 Conclusions

A radiotracer investigation was successfully undertaken to investigate the flow dynamics of clinkers in a ball mill of a cement production plant in Kenya. The residence time distribution for mill 1 was measured for two runs. It was demonstrated that technetium-99m, obtained from a molybdenum-technetium generator meant for healthcare applications, can be used as a radiotracer for tracing the clinker flow in a ball mill. More specifically, a Tc-99m concentration of 2,000 MBq or higher is adequate to conduct RTD measurements of clinker milling operations. This is especially significant for Kenya and other developing countries, where radioisotopes produced from reactors are not readily available.

It was noted that one of the NaI(Tl) scintillation detectors, D2, was recording higher background radiation levels at the outlet of the mill, an average of 79 counts per second versus 22 and 18 counts per second recorded by detectors D1 and D3 respectively. This background reading however remained stable throughout the investigation and might be attributed to higher traces of adsorped heavy metals in the mill outlet.

The MRT of clinker feed was determined to be 980.5 s from the average of the two runs, whereas the clinker holdup was estimated to be 13.6 tonnes within the ball mill. The MRTs of the clinkers within the separator and the entire milling circuit were found to be 44.5 s and 1025 s, respectively. The hold-up of the mill from the two runs was consistent and was determined to be 13.6 tonnes.

The experimental data was modelled using DTS PRO software and the data was found to fit two models; Axial dispersion and tank-in-series with back-mixing models connected with a plug flow component in series were found sufficient, to characterize the flow of solids within the mill. The two models revealed a significant degree of axial dispersion (back-mixing) within the ball mill, which is not preferable for the efficient operation of the ball mill. No other malfunctioning or flow abnormality such as bypassing or channelling of flow was observed.

### 5.2 Recommendations

It is recommended that the results of the study be utilized to evaluate the performance and optimize the operating parameters of the ball mill. Further, the results could be used to modify the design of the mill to minimize the observed back-mixing thereby increasing process efficiency. A follow-up RTD measurement should be carried out to confirm that the back-mixing has been eliminated and quantify the effect of back-mixing on grinding efficiency. The cause of the higher background levels at the mill outlet should also be investigated.

Due to its availability locally, Tc-99m can be used to study more industrial processes especially those with short residence times.

## References

- Adwet, W.M., Pant, H.J., Mangala, M.J., Masinza, S.A., 2019. Evaluation of hydraulic performance of an anaerobic pond using radiotracer technique. *Applied Radiation and Isotopes* 145, 101–105.  
<https://doi.org/10.1016/j.apradiso.2018.12.017>
- Adzaklo, S. Y., Dagadu, C. P. K., Adu, P. S., & Affum, H. A. (2016). *Investigation of Feed Dynamics in Clinker Grinding Mill by Residence Time Distribution Method*. 8.
- Alsop, P. A. (2007). *Cement Plant Operations Handbook: For Dry Process Plants*.
- Abdelouahed, H. B., & Reguigui, N. (2011). Radiotracer investigation of phosphoric acid and phosphatic fertilizers production process. *Journal of Radioanalytical and Nuclear Chemistry*, 289(1), 103–111.
- Abdelouahed, H. B., Pant, H. J., Thereska, J., Abbes, N. E., & Reguigui, N. (2018). Investigation of flow dynamics of phosphate fertilizer production reactors using radiotracer technique. *Applied Radiation and Isotopes*, 142, 143–150. <https://doi.org/10.1016/j.apradiso.2018.09.015>
- Austin, L.G., Luckie, P.T., Ateya, B.G. (1971). Residence time distributions in mills. *Cement and Concrete Research* 1, 241–256.
- Bjørnstad, T., Garder, K., Hundere, I., & Michelsen, O. B. (1990). Tracer Tests in Oil Appraisal and Reservoir Evaluation: State of the Art. In A. T. Buller, E. Berg, O. Hjelmeland, J. Kleppe, O. Torsæter, & J. O. Aasen (Eds.), *North Sea Oil and Gas Reservoirs—II* (pp. 261–270). Springer Netherlands.
- Bye, G. C. (1999). *Portland Cement: Composition, Production and Properties*. Thomas Telford.
- Canadian Nuclear Safety Commission. (2017). *Radionuclide information booklet*.
- Charlton, J.S., (1984). Radioisotope Techniques for Problem-Solving in the Chemical Industry. Proceedings of the Institution of Mechanical Engineers, Part A: Power and Process Engineering 198, 81–88.
- Charlton, J. S. (2012). *Radioisotope Techniques for Problem-Solving in Industrial Process Plants*. Springer Science & Business Media.
- Cleary, P. W. (2006). *Axial transport in dry ball mills*. <https://doi.org/10.1016/j.apm.2006.03.018>
- Danckwerts, P. V. (1953). Continuous flow systems. *Chemical Engineering Science*, 2(1), 1–13.



- Daruich de Souza, C., Nogueira, B.R., Zeituni, C.A., Rostelato, M.E.C.M., (2022). Chapter 15 - Radioactive nanoparticles and their biomedical application in nanobrachytherapy, in: Kesharwani, P., Singh, K.K. (Eds.), *Nanoparticle Therapeutics*. Academic Press, pp. 529–560.
- De Clercq, J., Jacobs, F., Kinnear, D. J., Nopens, I., Dierckx, R. A., Defrancq, J., & Vanrolleghem, P. A. (2005). Detailed spatio-temporal solids concentration profiling during batch settling of activated sludge using a radiotracer. *Water Research*, 39(10), 2125–2135.
- Du Plessis, H., Kearsley, E., & Matjie, H. (2007). *Effect of grinding time on the particle size distribution of gasification ash and Portland cement clinker*. ResearchGate. Retrieved February 20, 2019, from
- Fogler, H. S. (2016). *Elements of Chemical Reaction Engineering*. Prentice Hall PTR.
- Gonçalves, M. C., & Margarido, F. (Eds.). (2015). *Materials for Construction and Civil Engineering*. Springer International Publishing.
- Goswami, S., Pant, H. J., Sheoran, M., Chandra, A., Sharma, V. K., & Bhunia, H. (2020). Residence time distribution measurements in an industrial-scale pulp digester using technetium-99m as radiotracer. *Journal of Radioanalytical and Nuclear Chemistry*, 323(3), 1373–1379.
- Group, O. B. (2015). *The Report: Kenya 2016*. Oxford Business Group.
- Hassanzadeh, A. (2017). Measurement and modeling of residence time distribution of overflow ball mill in continuous closed circuit. *Geosystem Engineering*, 20(5), 251–260.
- Hewlett, P. (2003). *Lea's Chemistry of Cement and Concrete*. Elsevier.
- Hidayati, N.R., 2016. Application of 99m Tc Radioisotope In Diagnostic Procedures And Internal Radiation Dose Estimation. KEn 1.
- Huang, Y., Seinfeld, J.H., 2019. A note on flow behavior in axially-dispersed plug flow reactors with step input of tracer. *Atmospheric Environment: X* 1, 100006.
- International Atomic Energy Agency. (2001). *Radiotracer technology as applied to industry: Final report of a co-ordinated research project 1997–2000*.
- International Atomic Energy Agency. (2004). *Radiotracer applications in industry: A guidebook*.

- International Atomic Energy Agency (2008). *The Radiotracer Residence Time Distribution Method for Industrial and Environmental Applications. Training Course Series 31.*
- International Commission on Radiological Protection (2007). *Annals of the ICRP: The 2007 Recommendations of the International Commission on Radiological Protection. ICRP Publication 103.*
- Kasban, H., Zahran, O., Arafa, H., El-Kordy, M., Elaraby, S. M. S., & Abd El-Samie, F. E. (2010). Laboratory experiments and modeling for industrial radiotracer applications. *Applied Radiation and Isotopes*, 68(6), 1049–1056.
- Kasban, H., Zahran, O. & El-Samie F.A. (2010). New Trends for On-Line Troubleshooting in Industrial Problems Using Radioisotopes. *The Online Journal on Electronics and Electrical Engineering*. 2.
- Knoll, G. F. (2010). *Radiation Detection and Measurement*. John Wiley & Sons.
- Kenya National Bureau of Statistics. (2018). *Economic Survey 2017*.
- Loveland, W. D., Morrissey, D. J., & Seaborg, G. T. (2005). *Modern Nuclear Chemistry*. John Wiley & Sons.
- Levenspiel, O. (1972). *Chemical reaction engineering* (2d ed). Wiley.
- Makokha, A., Starovoytova, D., Namango, S., & Ataro, E. (2014). Effect of Slurry Solids Concentration and Ball Loading on Mill Residence Time Distribution. *Journal of Mining Engineering and Mineral Processing* 3. 21-27. 10.5923/j.mining.20140302.01.
- Michelsen, M. L. (1972). A least-squares method for residence time distribution analysis. *The Chemical Engineering Journal*, 4(2), 171–179. [https://doi.org/10.1016/0300-9467\(72\)80008-X](https://doi.org/10.1016/0300-9467(72)80008-X)
- Mohd Yunos, M.A.S., (2016). Industrial Radiotracer Technology for Process Optimizations in Chemical Industries. *The Pertanika Journal of Scholarly Research Reviews* 2, 20–46.
- Mumuni, I.I., Rasheed, N. A., Nordin, M. J., Dakheel, A. H., Nados, W. L., & Maarroof, M. K. A. (2017). Research Journal of Applied Sciences, Engineering and Technology. *Research Journal of Applied Sciences, Engineering and Technology*, 14(9), 324–333. <https://doi.org/10.19026/rjaset.14.5072>
- National Cement Company Limited (2018). *2018 Half Year Production Report*.
- Olsen, D., Goli, S., Faulkner, D., & McKane, A. (2010). *Opportunities for Energy Efficiency and Demand Response in the California Cement Industry* (LBNL-4849E, 1050705; p. LBNL-4849E, 1050705). <https://doi.org/10.2172/1050705>

- Othman, N., & Kamarudin, S. K. (2014). Radiotracer Technology in Mixing Processes for Industrial Applications. *The Scientific World Journal*, 2014, 1–15. <https://doi.org/10.1155/2014/768604>
- Pant, H. J., Kundu, A., & Nigam, K. D. P. (2001). RADIOTRACER APPLICATIONS IN CHEMICAL PROCESS INDUSTRY. *Reviews in Chemical Engineering*, 17(3).  
<https://doi.org/10.1515/REVCE.2001.17.3.165>
- Pant, H. J., Goswami, S., Samantray, J. S., Sharma, V. K., & Maheshwari, N. K. (2015). Residence time distribution measurements in a pilot-scale poison tank using radiotracer technique. *Applied Radiation and Isotopes*, 103, 54–60. <https://doi.org/10.1016/j.apradiso.2015.05.016>
- Pant, H. J., Sharma, V. K., Shenoy, K. T., & Sreenivas, T. (2015). Measurements of liquid phase residence time distributions in a pilot-scale continuous leaching reactor using radiotracer technique. *Applied Radiation and Isotopes*, 97, 40–46. <https://doi.org/10.1016/j.apradiso.2014.12.010>
- Plasari, E., Thereska, J., LecIerc, J.R., & Villermaux, J., (1999). Tracer Experiments and Residence-Time Distributions in the Analysis of Industrial Units: Case Studies, *Nukleonika*, Vol. 44, No. I, 39-58.
- Progepi/Sysmatec, 2000. *Instruction Manual of RTD Analysis Software, DTS Pro, V.4.2.*
- Rogers, R. S. C., & Austin, L. G. (1984). RESIDENCE TIME DISTRIBUTIONS IN BALL MILLS. *Particulate Science and Technology*, 2(2), 191–209. <https://doi.org/10.1080/02726358408906404>
- Sheoran, M., Goswami, S., Pant, H. J., Biswal, J., Sharma, V. K., Chandra, A., Bhunia, H., Bajpai, P. K., Rao, S. M., & Dash, A. (2016). Measurement of residence time distribution of liquid phase in an industrial-scale continuous pulp digester using radiotracer technique. *Applied Radiation and Isotopes*, 111, 10–17.  
<https://doi.org/10.1016/j.apradiso.2016.01.025>
- Sheoran, M., Chandra, A., Bhunia, H., Bajpai, P. K., & Pant, H. J. (2018). Residence time distribution studies using radiotracers in chemical industry—A review. *Chemical Engineering Communications*, 205(6), 739–758. <https://doi.org/10.1080/00986445.2017.1410478>
- The European Cement Association, (2016). *Activity Report 2015*. The European Cement Association.
- Thýn, J., & Žitný, R. (2002). *Analysis and Diagnostics of Industrial Processes by Radiotracers and Radioisotope Sealed Sources*. Vydavatelství ČVUT.

Vinnett, L., Contreras, F., Lazo, A., Morales, M., Díaz, F., & Waters, K. E. (2018). The use of radioactive tracers to measure mixing regime in semi-autogenous grinding mills. *Minerals Engineering*, 115, 41–43.

<https://doi.org/10.1016/j.mineng.2017.10.006>

Worrell, E., & Galitsky, C. (2008). *Energy Efficiency Improvement and Cost Saving Opportunities for Cement Making. An ENERGY STAR Guide for Energy and Plant Managers* (LBNL-54036-Revision, 927882).

<https://doi.org/10.2172/927882>

Zahran O., Kasban H., Arafa H., El-Kordy M., & Abd El-Samie F.E. (2009). *Residence time distribution measurements in phosphate production unit using radiotracer techniques, in: 48th Annual British Conference on Non-Destructive Testing.*